

**Integrated Lifting-Surface and Euler/Boundary-Layer Theory  
Analysis Method for Marine Propulsors**

by

Christopher J. Hanson

B.S., Naval Architecture, U.S. Naval Academy, 1993

Submitted to the Departments of Ocean Engineering and Mechanical Engineering  
in partial fulfillment of the requirements for the degrees of

Naval Engineer

and

Master of Science in Mechanical Engineering

at the

MASSACHUSETTS INSTITUTE OF TECHNOLOGY

February 2001


© Christopher J. Hanson, 2000. All rights reserved.

The author hereby grants to MASSACHUSETTS INSTITUTE OF TECHNOLOGY permission to reproduce and to  
distribute copies of this thesis document in whole or in part.

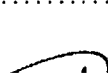
Signature of Author .....

Departments of Ocean Engineering and Mechanical Engineering  
13 December 2000

Certified by .....

 Justin E. Kerwin  
Professor of Naval Architecture  
Thesis Supervisor


Read by .....

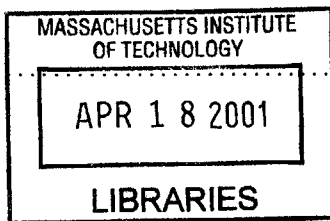
 Douglas P. Hart  
Associate Professor of Mechanical Engineering  
Thesis Reader

Accepted by .....

Nicholas M. Patrikalakis  
Kawasaki Professor of Engineering  
Chairman, Committee on Graduate Students  
Department of Ocean Engineering

Accepted by .....

 Ain A. Sonin  
Chairman, Committee on Graduate Students  
Department of Mechanical Engineering



BARKER

**Integrated Lifting-Surface and Euler/Boundary-Layer Theory Analysis  
Method for Marine Propulsors**

by

Christopher J. Hanson

Submitted to the Departments of Ocean Engineering and Mechanical Engineering  
on 13 December 2000, in partial fulfillment of the  
requirements for the degrees of  
Naval Engineer  
and  
Master of Science in Mechanical Engineering

**Abstract**

A propeller lifting surface design and analysis program is automatically coupled with an Euler / Integrated Boundary Layer Theory (IBLT) axisymmetric flow solver. The lifting surface method solves the localized propeller problem, while the Euler/IBLT solver handles the global flowfield, capturing the effective inflow problem. For viscous flows, the boundary layer is constructed based upon the parameters specified by the IBLT solution, and is merged with the inviscid Euler flowfield. The robust coupled method is capable of representing open propellers, ducted propulsors, and internal flow cases, including multi-blade row applications. For large axisymmetric bodies, the user may specify a nominal inflow, and the coupled method is used for the localized propulsor problem only, further increasing the computational efficiency. The specified nominal flow field may be calculated by other numerical flow solvers, obtained from experimental results, or calculated from a Euler/IBLT solution of the entire body. The coupled code is an extremely rapid flowfield gridding, calculation, and convergence method, which allows an order of magnitude reduction in convergence time when compared to the current efforts using Reynolds Averaged Navier Stokes (RANS) as the flow solver. Experimental validation is demonstrated for open, ducted, and internal flow propulsors.

Thesis Supervisor: Justin E. Kerwin  
Title: Professor of Naval Architecture

# Acknowledgments

For Catherine, a supportive wife, and Caroline, a joyous daughter.

Thanks to Professor Justin Kerwin and Dr. Todd Taylor for their assistance, ideas, and periodic nudges in the right direction.

Support for this research was provided by the Office of Naval Research under contract N00014-95-1-0369.

# Contents

<b>1</b>	<b>Introduction</b>	<b>12</b>
1.1	Overview . . . . .	12
1.2	Lifting-Surface Propeller Blade Design and Analysis . . . . .	12
1.3	Euler/IBLT Throughflow Solver . . . . .	14
1.3.1	Euler Throughflow Solver . . . . .	15
1.3.2	Integral Boundary Layer Theory Equations . . . . .	16
1.3.3	MTFLOW Operation . . . . .	18
1.4	Objective . . . . .	18
<b>2</b>	<b>Coupling PBD to MTFLOW</b>	<b>19</b>
2.1	Process Overview . . . . .	19
2.2	Running the Coupling . . . . .	20
<b>3</b>	<b>PBD to MTFLOW Conversions</b>	<b>23</b>
3.1	Program Overview . . . . .	23
3.2	Program Operation . . . . .	23
3.2.1	Program Flow and Required Files . . . . .	23
3.2.2	The tflow.xxx file . . . . .	24
3.2.3	Calculation of the Normalized Streamfunction . . . . .	26
3.2.4	Tflow.xxx Construction . . . . .	28
3.3	Multi-Blade Row Method . . . . .	29
3.4	Upstream Boundary Layer . . . . .	31
3.4.1	Velocity to Entropy Conversion . . . . .	32

3.4.2	Boundary Layer Entropy Modeling on Submerged Body . . . . .	34
3.4.3	Gridding Requirements for Stern Section Modeling . . . . .	35
<b>4</b>	<b>MTFLOW to PBD Conversions</b>	<b>41</b>
4.1	Program Overview . . . . .	41
4.2	Program Operation . . . . .	41
<b>5</b>	<b>Validation</b>	<b>46</b>
5.1	Open Propeller . . . . .	46
5.2	Ducted Propeller . . . . .	47
5.3	WaterJet . . . . .	50
5.4	Submerged Body . . . . .	51
<b>6</b>	<b>Conclusions</b>	<b>54</b>
6.1	Summary of Results . . . . .	54
6.2	Recommendations for Future Work . . . . .	54
<b>A</b>	<b>Multi-Blade Row Script File Examples</b>	<b>56</b>
A.1	BatchFile . . . . .	56
A.2	RunMTFLO . . . . .	60
A.3	RunMTSOL . . . . .	60
A.4	velcon.rot . . . . .	60

# List of Figures

1-1	Finite volume geometry for throughflow solver[2]. . . . .	15
2-1	Coupling sequence between propeller blade design code (PBD) and the throughflow solver (MTFLOW). . . . .	20
3-1	Program order and file passing when running PBD to MTFLOW. The end product is the ascii file tflow.xxx, which is the required input for MTFLO. . . . .	24
3-2	Streamline tracing required to find nondimensional streamline number for any given point of interest in the flow field. . . . .	27
3-3	Field parameter $s, t$ grid for an open propeller on a straight shaft, showing doubled $t$ profiles at blade leading and trailing edge. . . . .	28
3-4	Sample grid demonstrating the relationship between the various parameters within PBD2MT. . . . .	29
3-5	Multiple blade row coupling directory structure and program flow chart. The process is best controlled by a batch script file. . . . .	30
3-6	Screen capture of MTFLO displaying the tflow.xxx file information for a rotor/stator waterjet. . . . .	31
3-7	Straight shaft with $\frac{1}{7}^{th}$ power law boundary layer specified by an entropy loss. . . . .	33
3-8	Program operation and file passing to scale the specified entropy loss to match the desired nominal profile at the propeller inlet plane. . . . .	36
3-9	MTFLOW and experimental nominal velocity comparison of Huang Body 1 at $X/L = 0.977$ with inlet entropy loss specified at $X/L = 0.914$ . . . . .	37

3-10	Resulting nominal velocity profile at $X/L = 0.914$ in MTFLOW with the required entropy loss to correctly match the nominal profile at the propeller location of $X/L = 0.977$ compared to experimental profile at $X/L = 0.914$ . . . . .	38
3-11	Nominal flow over stern section of Huang Body 1 with inlet boundary layer modeled as an entropy loss. . . . .	39
3-12	Grid comparison showing drift of bottom left corner (top) when inlet body points entered at actual location versus adjusted body points (bottom). . . . .	40
4-1	Program order and file passing when running MTFLOW to PBD. The end product is the TECPLOT format file restart.vel (or other name as specified during VELCON execution), which is the required input for PBD. . . . .	42
4-2	Sample viscous flowfield output from MTFLOW. . . . .	44
4-3	Sample BL2BODY grid with boundary layer reconstruction grid added to the inviscid MTFLOW grid. . . . .	44
4-4	Comparison of reconstructed boundary layer profile and experimental measurements for Huang Body 1. As expected, the accuracy of the $\frac{1}{7}^{th}$ power law diminishes in the highly tapered stern region. . . . .	45
5-1	Contour plot of the effective axial velocity in the presense of a uniform nominal inflow velocity of 1.0 for P4119 on an inviscid straight shaft. . . . .	48
5-2	Comparison of the circumferential mean tangential velocity at the blade trailing edge of P4119 from MTFLOW and PBD. . . . .	48
5-3	Comparison of P4119 MTFLOW/PBD results with 1998 ITTC Experiment. PBD was run with both sectional drag coefficients and thickness effects included and with a vorticy grid lattice of 35 x 35. . . . .	49
5-4	Kaplan KA-455 ducted propulsor as modeled in PBD. . . . .	49
5-5	Contour plot of circumferential mean tangential velocity of WaterJet WJ21 with streamlines superimposed. Flow is from left to right. The rotor leading edge is located at approximatly $X = 0.2$ and the stator leading edge is located at approximatly $X = 1.0$ . . . . .	50
5-6	Representation of Huang Body 1 (DTMB Model 5225-1). . . . .	51

5-7 Huang Body 1 nominal and effective velocity comparison of MTFLOW and experiment at  $X/L = 0.977$  with inlet entropy loss specified at  $X/L = 0.914$ . The propeller leading edge tip is located at  $R = 0.545$ . . . . . 52



# List of Tables

2.1	Coupling code description . . . . .	21
2.2	Example coupling administration file . . . . .	21
3.1	Input files required by the program PBD2MT. . . . .	24
3.2	Example tflow.xxx input file to MTFLO . . . . .	25
3.3	Required format of boundary layer file. The number of points in the boundary layer are listed in the first line, followed by each R, V point, where V is the axial velocity component. . . . .	35
5.1	Comparison of KA-455 inviscid and viscid MTFLOW/PBD rotor results with experimental data at design $J=0.36$ . . . . .	49
5.2	Comparison of waterjet WJ21 MTFLOW/PBD and RANS/PBD results with experimental data. . . . .	51
5.3	Comparison of propeller 4577 performance on Huang Body 1 with $J = 1.25$ . . . .	53

# Nomenclature

$A$		streamtube cross sectional area
$A_1, A_2$		area vector normal to streamtube volume along streamtube
$B$		number of blades
$B^-, B^+$		area vector normal to streamtube
$C_f$		skin friction coefficient
$D$		propeller diameter
$H$		boundary layer shape parameter
$h_o$		stagnation enthalpy
$J$	$\frac{V_s}{nD}$	advance coefficient
$K_T$	$\frac{T}{\rho n^2 D^4}$	thrust coefficient
$K_Q$	$\frac{Q}{\rho n^2 D^5}$	torque coefficient
$L$		vehicle length
$L_{ref}$		reference length
$M$		Mach number
$\hat{n}$		surface normal vector
$n$		propeller rotation rate ( $\frac{rev}{sec}$ )
$p$		pressure
$p_o$		absolute total pressure
$Q$		mass flow rate
$r$		radial coordinate
$R_{max}$		local maximum flowfield radius
$R_{min}$		local minimum flowfield radius
$rV_\theta$		tangential swirl
$\hat{s}$		unit vector in direction of $v_m$
$S$		entropy
$t$		nondimensional streamline number
$T_\theta$		circumferential blade thickness
$u$		axial velocity component

$U_e$	boundary layer edge velocity
$\vec{V}_{effective}$	effective velocity
$\vec{V}_{induced}$	induced velocity
$v_m$	meridional velocity
$V_{ship}$	ship velocity
$\vec{V}_{total}$	total velocity
$v_\theta$	tangential (swirl) velocity
$x$	longitudinal coordinate
$y$	vertical coordinate
$z$	longitudinal coordinate
$Z$	number of propeller blades
$\delta$	boundary layer thickness
$\delta r$	radial difference from point of interest to a given streamline
$\delta_{99}$	boundary layer thickness at which $u = 0.99U_e$
$\delta^*$	boundary layer displacement thickness
$\Delta S$	added entropy
$\Delta W$	work addition
$\gamma$	specific heat ratio
$\Gamma$	blade circulation
$\Omega$	blade rotation rate ( $\frac{rad}{sec}$ )
$\rho$	fluid density
$\Pi$	streamtube normal pressure
$\theta$	boundary layer momentum thickness
$\tau_w$	wall shear stress
$\psi$	streamfunction

# Chapter 1

## Introduction

### 1.1 Overview

The goal of this research was the creation of a fully automatic coupled method between a lifting surface propeller blade design and analysis program and an Euler throughflow solver. A coupled technique is necessary as the propeller influences the flowfield, and the flowfield influence the propeller. Thus, both the propeller and flow field calculation must be iteratively converged to a final solution. Currently, coupled design and analysis of marine propulsors is generally accomplished by using a Reynolds Average Navier - Stokes (RANS) flow solver, the use of which is a computational intensive task requiring a high degree of operator knowledge and experience. A Euler solver with an Integral Boundary Layer Theory (IBLT) boundary layer reconstruction routine, enables solution convergence twenty to thirty times as fast as the current RANS methods.

### 1.2 Lifting-Surface Propeller Blade Design and Analysis

The use of lifting surface theory for the design and analysis of propellers has been extensively documented in the literature, and will be only summarized here for the sake of completeness[3],[11],[12]. Propeller Blade Design (PBD-14) developed by Kerwin<sup>1</sup> et al was used for this research. A lattice of discrete vortex segments is placed along the blade mean camber surface, the hub, the

---

<sup>1</sup>Justin E. Kerwin, Profesor of Naval Architecture, Ocean Engineering Department, MIT.

duct, if present, and the trailing wake system. Control points are placed a particular point within each grid lattice. Each lattice segment has an appropriate vorticity strength, such that the kinematic boundary conditions are satisfied along the gridded surface, namely the total velocity must be tangent to the surface at each control point.

In propeller design and analysis, the velocity relation is

$$\vec{V}_{total} = \vec{V}_{induced} + \vec{V}_{effective} \quad (1.1)$$

where

- $\vec{V}_{total} \equiv$  the total velocity in the presence of an operating propeller
- $\vec{V}_{induced} \equiv$  the velocity induced by the propeller and trailing wake vortex distributions
- $\vec{V}_{effective} \equiv$  the velocity due to the interaction between the propeller vortex distributions and the presence of vorticity in the inflow

and

$$\vec{V}_{nominal} \equiv \text{the velocity present in the absence of the propeller}$$

It is important to realize that neither  $\vec{V}_{induced}$  nor  $\vec{V}_{effective}$  are physical velocities that may be measured. Only  $\vec{V}_{total}$  actually exists in the flow field, and its division into two components is done solely for computational reasons. It is important to point out that the above listed velocities are completely independent from the nominal velocity  $\vec{V}_{nominal}$  which is the velocity present in the absence of the propeller. Based on the above definitions, it is useful to note that if no vorticity is present in the nominal flowfield, then no interaction between the propeller, as modeled by vortex distributions, and the inflow are necessary. Thus, *in this special case*, the nominal inflow is equal to the effective inflow. This is never the case in reality since viscous effects are always present, however it often serves as a useful check of propeller analysis code operation when run in an inviscid mode.

The lifting surface method solves the propeller problem by first developing an influence

matrix  $[INF]$  which gives the velocity induced by each vortex lattice segment, with an assumed unit strength, upon each control point. When this influence matrix is multiplied by the actual vortex segment strength, the induced velocity at every control point is known.

$$[INF] [\vec{\Gamma}] = \vec{V}_{induced} \quad (1.2)$$

The kinematic boundary condition is specified by dictating that the total velocity normal to the grid surface must be zero. Thus, for a zero thickness case,

$$[[INF] [\vec{\Gamma}] + \vec{V}_{effective}] \cdot \hat{n} = 0 \quad (1.3)$$

A lifting surface code may be used for either a design of a new propeller or an analysis of an existing propeller. In both cases, Equation 1.3 applies, only the knowns versus unknowns vary. In the case of propeller design, a desired radial and chordwise loading distribution is prescribed, and the blade shape is manipulated until Equation 1.3 is satisfied. In propeller analysis, the blade shape is prescribed, and the resulting circulation is solved. Blade thickness effects are added by placing discrete source lines coincident with the spanwise blade vortex lines. The resulting propeller forces due to the lifting surface and thickness are calculated from the Kutta-Joukowski and Lagally theorems, respectively. A leading edge suction force and Lighthill pressure distribution correction are applied to those forces, and the propeller's sectional viscous drag is calculated based on either stripwise two-dimensional empirical drag coefficients or a stripwise two-dimensional integral boundary layer calculation.

### 1.3 Euler/IBLT Throughflow Solver

MTFLOW is a Euler/IBLT throughflow solver developed by Drela<sup>2</sup>. MTFLOW incorporates a streamline curvature method is a powerful method for solving the inviscid flowfield within a channel or annular passage. As the method is inviscid, a boundary layer solution must be used to calculate boundary layer quantities. The inviscid streamlines are then displaced off the body by the displacement thickness,  $\delta^*$ , which causes a redistribution of the inviscid streamlines.

---

<sup>2</sup>Mark Drela, Associate Professor, Department of Aeronautics and Astronautics, MIT

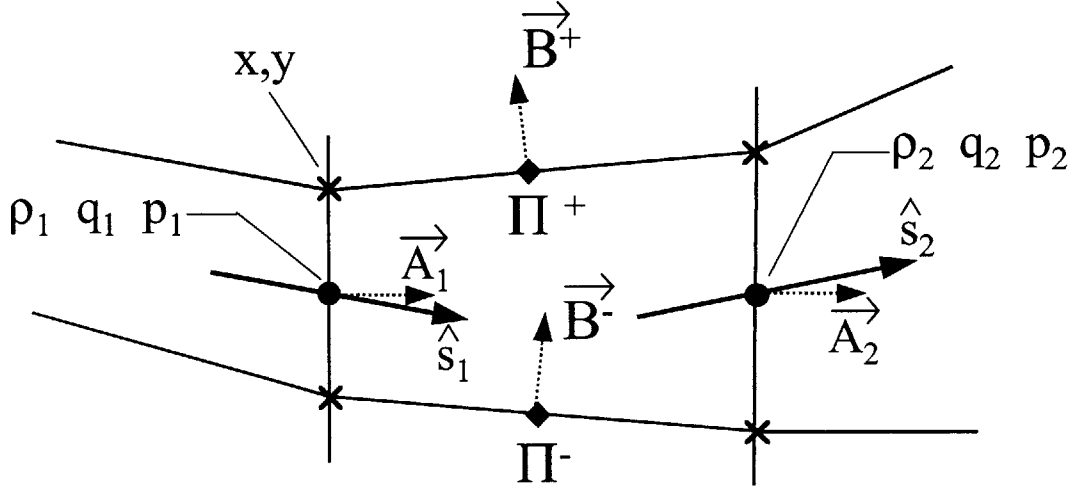


Figure 1-1: Finite volume geometry for throughflow solver[2].

### 1.3.1 Euler Throughflow Solver

MTFLOW is based on the conservative formulation of the steady state Euler equations[1]. It relies on a finite-volume throughflow method based on the streamline curvature method. Figure 1-1 displays the finite-volume geometry representation used within MTFLOW.

The first governing equation is the conservation of mass. Thus, across adjacent finite volume boundaries

$$\rho_1 v_{m1} \hat{s}_1 \cdot \vec{A}_1 = \rho_2 v_{m2} \hat{s}_2 \cdot \vec{A}_2 \quad (1.4)$$

The conservation of momentum is written as the steady state Euler equation.

$$P_1 \vec{A}_1 + (\rho_1 v_{m1} \hat{s}_1 \cdot \vec{A}_1) v_{m1} \hat{s}_1 + \Pi^- \vec{B}^- = P_2 \vec{A}_2 + (\rho_2 v_{m2} \hat{s}_2 \cdot \vec{A}_2) v_{m2} \hat{s}_2 + \Pi^+ \vec{B}^+ \quad (1.5)$$

Conservation of energy is solved in terms of enthalpy

$$\frac{\gamma}{\gamma-1} \frac{P_1}{\rho_1} + \frac{1}{2} v_{m1}^2 = \frac{\gamma}{\gamma-1} \frac{P_2}{\rho_2} + \frac{1}{2} v_{m2}^2 \quad (1.6)$$

Additionally the average pressures along the faces pseudo-normal to and along the streamtube must be equal.

$$P_1 + P_2 = \Pi^+ + \Pi^- \quad (1.7)$$

MTFLOW further simplifies equations 1.4 through 1.7. The meridional flow speed,  $v_m$  is obtained from a local streamtube conservation of mass.

$$v_m = \frac{Q}{\rho A(2\pi r - BT_\theta)} \quad (1.8)$$

The streamwise momentum equation solved by MTFLOW is of the same form as Equation 1.4.

$$dP + \rho v_m dv_m + \rho v_\theta dv_\theta + Pd(\Delta S) - \rho d(\Delta W) = 0 \quad (1.9)$$

The change in work, say due to the presence of a propeller,  $\Delta W$  enters the formulation through the Euler turbine equation.

$$\Delta W = \int \Omega d(rv_\theta) \quad (1.10)$$

with

$$\Omega \equiv \text{blade rotation rate } \left(\frac{\text{rad}}{\text{sec}}\right)$$

This results in a computationally efficient methodology for solving the inviscid equations of motion, and is ideally suited to couple with the propeller lifting surface code PBD.

### 1.3.2 Integral Boundary Layer Theory Equations

Laminar and turbulent boundary layer flows are governed by the same integral momentum equation, obtained by integrating a combination of the continuity and simplified  $x$ -momentum equations term by term across the boundary layer [17]:



$$\frac{d\theta}{dx} + (2 + H)\frac{\theta}{U_e}\frac{dU_e}{dx} = \frac{C_f}{2} \quad (1.11)$$

where

$$\theta = \text{momentum thickness} = \int_0^\infty \frac{u}{U_e} \left(1 - \frac{u}{U_e}\right) dy \quad (1.12)$$

$$\delta^* = \text{displacement thickness} = \int_0^\infty \left(1 - \frac{u}{U_e}\right) dy \quad (1.13)$$

$$H = \text{momentum shape factor} = \frac{\delta^*}{\theta} \quad (1.14)$$

$$\tau_w = \text{wall shear stress} = \rho\nu \frac{\partial u}{\partial y} \Big|_w \quad (1.15)$$

$$C_f = \text{skin friction coefficient} = \frac{2\tau_w}{\rho U_e^2} \quad (1.16)$$

In laminar flow, the variables  $\theta$ ,  $H$ , and  $C_f$  can be reasonably well related with one-parameter velocity profile approximations. For marine vehicles moving at typical speeds, however, the transition from laminar to turbulent flow within the boundary occurs near the bow, and the boundary layer remains turbulent over the remainder of the vehicle. The turbulent-flow profile is complicated in shape, and many different correlations or additional relations have been proposed to effect closure of Equation 1.11 [17]. The closure relations used within MTFLOW are those derived by Swafford[15]. It is important to note again however, that MTFLOW does not solve for the boundary layer velocity profile, but rather computes the boundary layer parameters and displaces the inviscid flow field off the body by  $\delta^*$ , and thus computes the global flow field inviscidly.

One of the simplest, and thus robust, approaches to express the boundary layer velocity profile and recommended for general use by White [17], is the  $\frac{1}{7}^{th}$  power law:

$$\frac{u}{U_e} = \left(\frac{y}{\delta_{99}}\right)^{1/7} \quad (1.17)$$

where  $\delta_{99}$ , the boundary layer thickness, is the value of  $y$  at which the boundary layer velocity is equal to 99 % of free stream velocity. By substituting Equation 1.17 into Equation 1.13 and replacing the upper limit of infinity of the integral with  $\delta_{99}$ , the relationship between  $\delta^*$  and  $\delta_{99}$  is:

$$\delta_{99} = 8\delta^* \quad (1.18)$$

This relation is useful to determine the boundary layer thickness given a known displacement thickness. Then Equation 1.17 may be used to determine  $u$  as a function of  $y$ .

### 1.3.3 MTFLOW Operation

MTFLOW consists of three executable programs; MTSET, MTFLO, and MTSOL. MTSET creates the body geometry and automatically sets up the initial grid. MTFLO allows the input of external flow field information, such as rotor generated swirl or additional losses, into the flow domain. MTSOL executes the flow field solution. The only required input file for MTFLOW is the `walls.xxx` file which is used by MTSET to define the body geometry. The creation of the `walls.xxx` file and the execution of the MTFLOW programs are sufficiently covered in Reference [1] and will thus not be repeated here. Hereafter, MTFLOW refers to the entire throughflow solver, while MTSET, MTFLO, and MTSOL refer to the individual running of the respective executable programs.

## 1.4 Objective

This thesis provides a description of the fully automated coupling between the throughflow solver MTFLOW and the lifting surface propeller blade design and analysis code PBD. An overview of the process is first presented, followed by more detailed descriptions of the coupling process. Finally, validation examples are presented.

## Chapter 2

# Coupling PBD to MTFLOW

### 2.1 Process Overview

The coupling of the lifting surface propeller blade design and analysis code and the streamline curvature code follows the same logic as utilized by Kerwin et al [9] when coupling the propeller blade design and analysis code with a RANS code. The basis of Kerwin's coupling was the use of distributed body forces within the RANS domain to represent the presence of the propeller. In the streamline curvature method, the propeller is modeled as a swirl introduction device. Thus added swirl, or angular momentum, is used to represent the presence of the propeller in the flowfield. This technique was first demonstrated by Renick [14] in a manual coupling method, and the present research is an extension of those efforts to produce a fully automated, robust method capable of solving the full range of propulsor types. While the overall concept and code execution is similar to that used by Renick, the coupling codes have been completely rewritten and additional changes have been incorporated into the flowfield solver to affect a correct and fully automatic coupling technique.

The coupling technique is started by solving the nominal flowfield, *i.e.* the body with no propeller present. For viscous flow, the boundary layer is reconstructed and merged to the flowfield. This nominal flow field is then passed to the lifting surface code which solves the localized propeller problem. The updated circumferential mean induced velocities are converted to swirl, and are then inserted into the global flowfield which is then reconverged. The process is then repeated until both the flowfield, and lifting surface propeller results have converged.

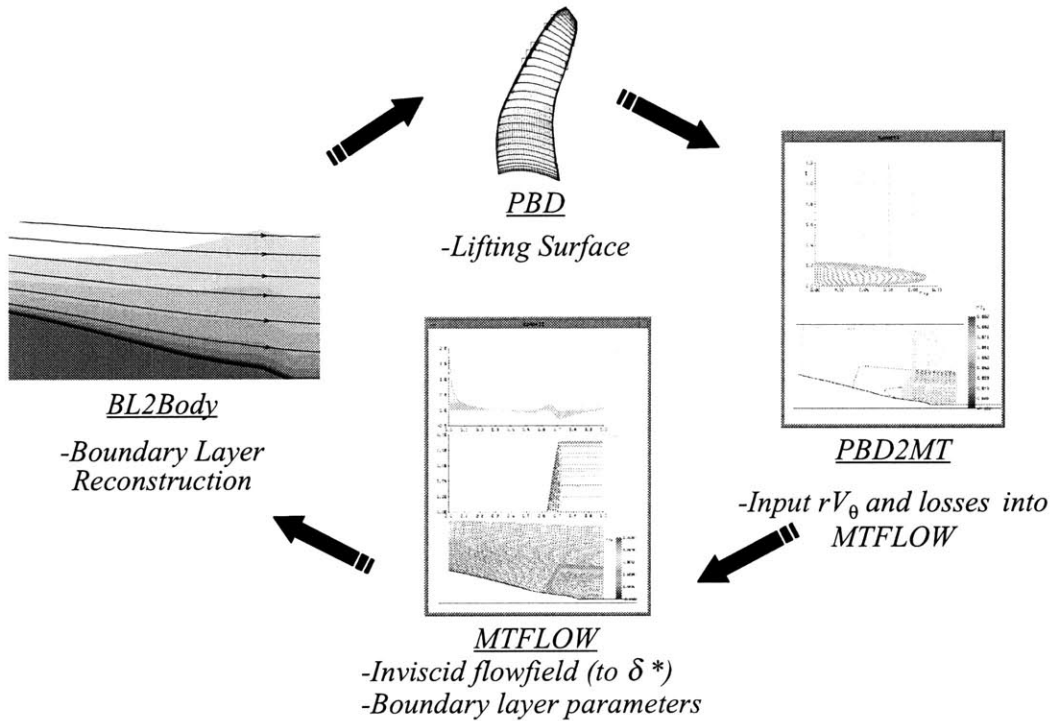


Figure 2-1: Coupling sequence between propeller blade design code (PBD) and the throughflow solver (MTFLOW).

The overall sequence is shown in Figure 2-1.

## 2.2 Running the Coupling

The overall coupling is controlled by the coupling administration file, `mtcouple.inp`. The coupling is executed by two computer codes: PBD2MT, which converts the PBD output to MTFLOW, and BL2BODY, which passes the updated flowfield to PBD. The codes are described in Table 2.1.

The coupling administration file, `mtcouple.inp`, contains the required conversion information to execute the coupling. A sample administration file is displayed in Table 2.2

The input lines have the following uses within the code:

1. REYNOLD'S NUMBER: Reynold's number for the throughflow domain. An inviscid

Code	Description
PBD2MT	1) Converts the PBD output circumferential mean induced velocity to swirl. 2) Writes out <code>tflow.xxx</code> , the input file to MTFLOW containing the induced $rV_\theta$ .
BL2BODY	1) Converts the MTFLOW output into velocity flowfield. 2) For viscous cases, reconstructs the boundary layer profile.

Table 2.1: Coupling code description

LINE 1:	3	!	Reynolds number
LINE 2:	0.01	!	inlet mach number
LINE 3:	1.0	!	Vship used in PBD to calculate Js
LINE 4:	2.0	!	x location of LE tip
LINE 5:	1.0	!	r location of LE tip
LINE 6:	xxx	!	MTFLOW case name
LINE 7:	xxx.pbd	!	pbid input file name
LINE 8:	1	!	BInput toggle (0=no,1=yes)
LINE 9:	0	!	Nominal velocity toggle (0=no,1=yes)
LINE 10:	2	!	Number of blade rows

Table 2.2: Example coupling administration file

case is forced by specifying a Reynold's number less than 10.

2. INLET MACH NUMBER: For compressible flows, the Mach number is defined as the inlet velocity divided by the speed of sound. For water,  $M = \frac{q}{1660 \frac{m}{sec}}$ . For general use with water a Mach number of 0.01 is recommended. This prevents round off errors internal to MTFLOW, and models the flow as virtually incompressible.
3. VSHIP: This is the upstream velocity at infinity. For coupling purposes it is the fluid velocity at the domain inlet. The advance coefficient,  $J$ , within PBD is calculated using  $V_{ship}$ . Traditionally cases are non-dimensionalized with  $V_{ship} = 1.0$ .
4. X LOCATION OF LE TIP: The axial location of the propeller leading edge tip in MTFLOW coordinates.
5. R LOCATION OF LE TIP: The radial location of the propeller leading edge tip in MTFLOW coordinates.
6. MTFLOW CASENAME: The casename of the walls geometry file read by MTSET. The generated state and `tflow.xxx` file will be automatically labeled with the casename

extension.

7. PBD INPUT FILE NAME: Name of the PBD administration file. Used to read the advance coefficient and number of blades.
8. BLINPUT TOGGLE: Specifies whether an inlet boundary layer profile is present. If set to 1, then the file `BLin.txt` is read, converted to entropy, and added to the flowfield.
9. NOMINAL VELOCITY TOGGLE: The toggle is set to 1 if the nominal profile is required for use in adjusting the specified input boundary layer to match a desired nominal profile at the plane of the propeller.
10. NUMBER OF BLADE ROWS: Specifies the total number of rotor and/or stator rows present in the propulsor. Thus, a value of 1 describes a traditional propeller, and a value of 2 is correct for a pre-swirl/rotor combination. Up to a total of nine blade rows are permitted.

## Chapter 3

# PBD to MTFLOW Conversions

### 3.1 Program Overview

Information is passed into MTFLOW by means of the `tflow.xxx` file. The `tflow` file may contain information for single blade rows, multiple blade rows, entropy loss due to the presence of an upstream boundary layer, or any combination of the above. This link of the coupling therefore requires the transfer of the necessary information into the `tflow` file. This is accomplished by the program PBD2MT.

### 3.2 Program Operation

#### 3.2.1 Program Flow and Required Files

After the successful execution of both MTFLOW to compute the nominal flowfield and the initial PBD run, PBD2MT is used to create the `tflow.xxx` file. As successive iterations are performed, grid information from the previous MTFLOW run, and the updated PBD output, are used to write an updated `tflow` file. By comparing the sizes of the various grid files, the program automatically determines the existence of an open, ducted, or internal flow propeller; and incorporates the necessary details into the `tflow` file. The required input files, source, and use, are explained in Table 3.1. The program operation is diagramed in Figure 3-1. The details of more complicated situations of multiple blade rows and inlet boundary layer profiles are described in later sections.

File	Source	Use
xxx.pbd	User	Uses propeller advance coefficient to compute rotation rate.
mtcouple.inp	User	Contains location of propeller in the flow domain and casename.
PBDOUT.CMV	PBD	Contains induced circumferential velocity.
Gridxxxxx.dat	MTSOL	Contains grid information from previous iteration used to compute nondimensional streamline numbers.

Table 3.1: Input files required by the program PBD2MT.

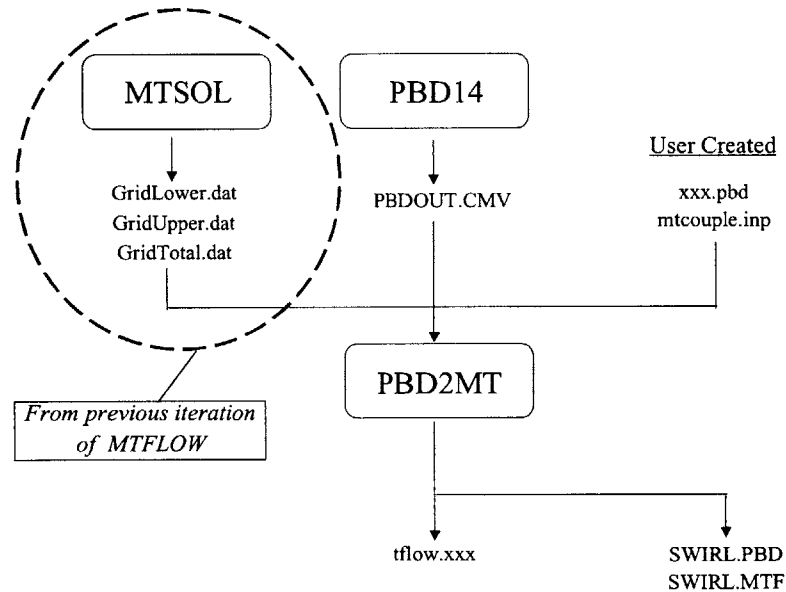


Figure 3-1: Program order and file passing when running PBD to MTFLOW. The end product is the ascii file `tflow.xxx`, which is the required input for MTFLO.

### 3.2.2 The `tflow.xxx` file

Information is passed into MTFLOW by use of the `tflow.xxx` file which is read by MTFLO. Prescribed distributions of  $rV_\theta$ ,  $\Delta S$ , etc., are specified as an  $M \times N$  grid of points arranged in a logical rectangle in the  $s, t$  parameter space. In the current coupling routine, only  $rV_\theta$  is specified in the file. The grid is input as a set of “profile blocks”. The grid is aligned with  $s$  the component perpendicular to the flow, and  $t$  the component parallel with the flow. Each block has a constant  $s$  value, and thus defines quantities as a profile perpendicular to the flow at that  $s$  value [1]. An example `tflow` file is shown in Table 3.2.



Label						
# t	z/L	r/L	rVt/qL	Thk/L	DS	DH/a <sup>2</sup>
# k	B	Omega L/q				
* 1.0	1.0	1.0	1.0	1.0	1.0	1.0
Kstage(1)	Nblade(1)	Omega(1)				
t(1,1)	X(1,1)	Y(1,1)	RVT(1,1)	THK(1,1)	DS(1,1)	DH(1,1)
t(2,1)	X(2,1)	Y(2,1)	RVT(2,1)	THK(2,1)	DS(2,1)	DH(2,1)
t(N,1)	X(N,1)	Y(N,1)	RVT(N,1)	THK(N,1)	DS(N,1)	DH(N,1)
.	.	.	.	.	.	.
Kstage(M)	Nblade(M)	Omega(M)				
t(N,M)	X(N,M)	Y(N,M)	RVT(N,M)	THK(N,M)	DS(N,M)	DH(N,M)

Table 3.2: Example tflow.xxx input file to MTFLO

The contents of the file are described below. Once again, items 11 and 12 are not determined in the current coupling technique, but are features which, in future work, may be utilized for further improvement. The reference length,  $L_{ref}$ , is defined as 1.0 in the MTFLOW coordinate system. The points are specified with  $n$  values increasing perpendicular to the flow, and  $m$  values increasing parallel to the flow.

1. LABEL: Arbitrary label text line.
2. # ...: Comment label lines.
3. \* 1.0 ...: Multiplier line which is applied to all subsequent values in the associated column. PBD2MT sets all multipliers at 1.0.
4. Kstage(m): Number of the rotor or stator stage which is described by the profile block. This MTFLOW function is not used in the coupling method, and is set to zero by PBD2MT.
5. Nblade(m): The number of blades present in the current s line.
6. Omega(m): The rotation rate in  $\Omega L_{ref}/q_{inl}$ .

7.  $t(n,m)$ : The normalized streamfunction  $t$ , described below.
8.  $X(n,m)$ : The  $x$  coordinate defined as  $z/L_{ref}$ .
9.  $Y(n,m)$ : The  $y$  coordinate defined as  $r/L_{ref}$ .
10.  $RVT(n,m)$ : The swirl defined as  $rV_\theta/q_{int}L_{ref}$ .
11.  $THK(n,m)$ : The blade thickness  $T_\theta/L_{ref}$ .
12.  $DS(n,m)$ : The added entropy  $\Delta S$  from some adiabatic loss process.
13.  $DH(n,m)$ : The added enthalpy  $\Delta H/a_{int}^2$  from heat release. ( Not applicable to propeller analysis.) This is always set to zero by PBD2MT.

### 3.2.3 Calculation of the Normalized Streamfunction

The normalized streamfunction,  $t$ , is defined as:

$$t = \bar{t}(\psi) \equiv \frac{\psi - \psi_1}{\psi_2 - \psi_1} \quad (3.1)$$

where, in the MTFLOW application,  $\psi_1$  and  $\psi_2$  are the streamfunction values at the innermost and outermost streamsurfaces of the flowpath between any two bodies, or elements, in the flowfield. With multi-element configurations,  $\psi_1$  and  $\psi_2$  are the streamfunction values at the bottom and top of one flow channel, and  $\bar{t}$  is additionally offset by the channel number, so that  $0 < t < 1$  between the first and second element,  $1 < t < 2$  between the second and third element, etc. In all situations, each streamsurface has a unique  $t$  value associated with it [1]. For a given  $z,r$  location, the normalized streamfunction may be calculated by:

$$t = \frac{\int_{R_{min}}^r \rho \pi r^2 dr}{\int_{R_{min}}^{R_{max}} \rho \pi r^2 dr} \quad (3.2)$$

which for uniform flow reduces to:

$$t = \frac{R^2 - R_{min}^2}{R_{max}^2 - R_{min}^2} \quad (3.3)$$

where

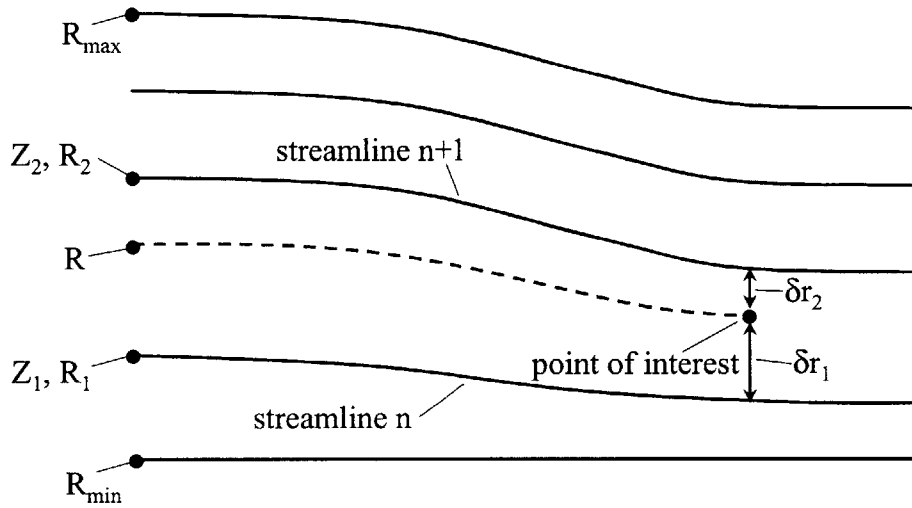


Figure 3-2: Streamline tracing required to find nondimensional streamline number for any given point of interest in the flow field.

$R$  = radius of point of interest

$R_{\min}$  = radius of bottom of local flow field

$R_{\max}$  = radius of top of local flow field

However, uniform flow generally only exists at the inlet of the MTFLOW domain. Thus, the following simple and robust approach is used to calculate the value of  $t$  given any  $z, r$  point of interest. The flowfield streamlines from the previous MTFLOW iteration are available in the `Gridxxx.dat` files. The applicable `Gridxxx.dat` file is selected, and the streamline above and below the point of interest is determined. The fractional difference between the point of interest and the identified streamlines, is traced back to the inlet, where uniform flow exists based on the inlet MTFLOW boundary conditions. Figure 3-2 shows the utilized streamline geometry. Thus the following equation is used to calculate  $R$ :

$$R = \frac{\delta r_1}{\delta r_1 + \delta r_2}(R_2 - R_1) + R_1 \quad (3.4)$$

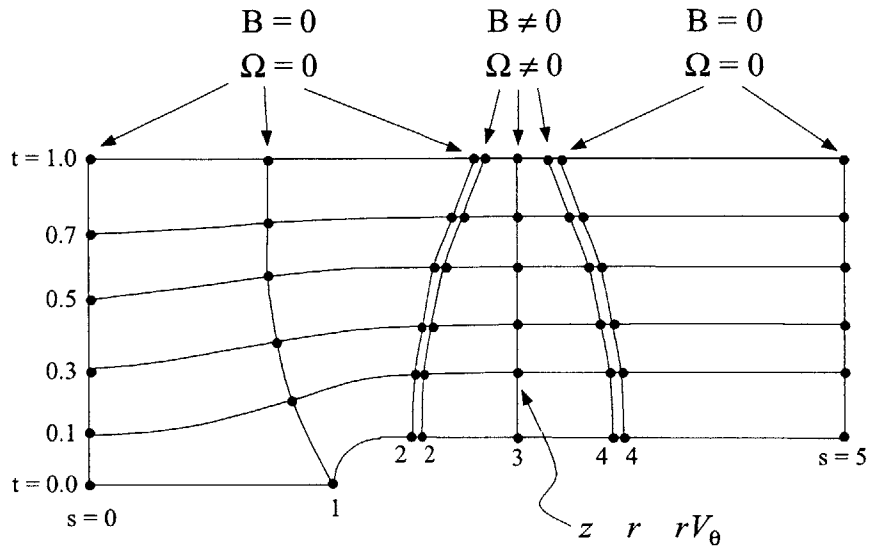


Figure 3-3: Field parameter  $s, t$  grid for an open propeller on a straight shaft, showing doubled  $t$  profiles at blade leading and trailing edge.

This calculated  $R$  value is then used in Equation 3.3 to determine the desired streamfunction,  $t$ , given any  $z, r$  position.

### 3.2.4 Tflow.xxx Construction

Figure 3-3 shows a general  $s, t$  grid for an open propeller on a straight shaft. To give more flexibility in splining, a slope break or discontinuity in either  $t$  or  $s$  can be specified by two identical  $t$ -value or  $s$ -value lines in each block of the `tflow.xxx` file. As shown in the example, the blade leading and trailing edge ( $s = 2$  and  $s = 4$ ) are doubled to force a spline break in  $B, \Omega$ , and  $rV_\theta$ . Thus two identical profile blocks with identical X, Y are generated. One with  $B, \Omega$ , and  $rV_\theta$  set to zero, and the other with  $B, \Omega$ , and  $rV_\theta$  set to the actual blade leading (or trailing) edge values. Similarly, a slope break or discontinuity in the  $s$  direction may be specified by two identical data lines within a given profile block. This is done at the blade tip, to enforce a zero  $rV_\theta$  condition outside the propeller.

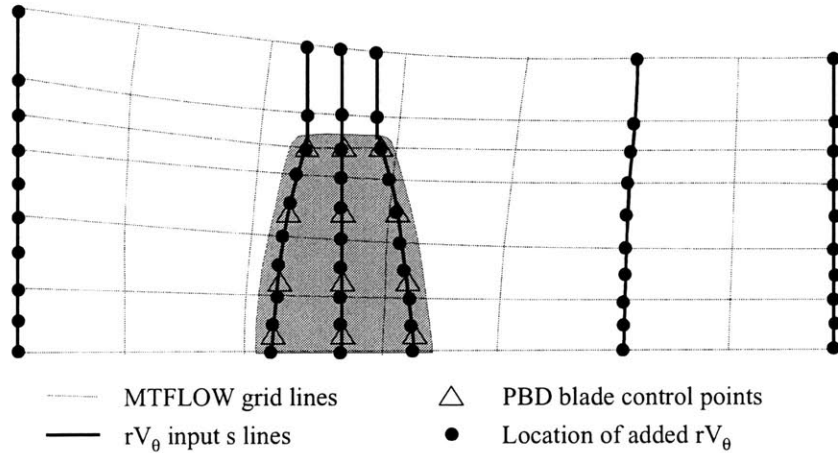


Figure 3-4: Sample grid demonstrating the relationship between the various parameters within PBD2MT.

### 3.3 Multi-Blade Row Method

In multiblade row applications, the induced  $rV_\theta$  from one blade row is convected in the wake to the next blade row, at which point the induced  $rV_\theta$  from the next blade are added to those in the wake from the upstream blade. Kelvin's theorem of conservation of circulation states that for any ideal fluid the circulation is constant along any streamline. Thus, lines of constant  $rV_\theta$  are convected along each streamline. Since the MTFLOW grid conforms to the streamlines, this coupling method is ideally suited for multiblade row applications. Individual `tflow.xxx` files are created for each blade row in their own subdirectory as described in Section 3.2.4. Each `tflow.xxx` is then moved to the master case directory and renamed based on the order of the blade rows. For example, the first blade row `tflow.xxx` file is renamed `tflow.B1`, the second blade row `tflow.xxx` file is renamed `tflow.B2`, etc. The program BUILDTFLOW then takes all the `tflow.Bx` files, determines the cumulative  $rV_\theta$  at each `s` line location, and creates the `tflow.casename` file containing all the blade row information. It is then this `tflow.xxx` file which is read by the program MTFLOW. The recommended directory structure and required file organization for a rotor/stator case is displayed in Figure 3-5. The program BUILDTFLOW can handle up to a total of nine blade rows. A script file for running a multi-blade row case is

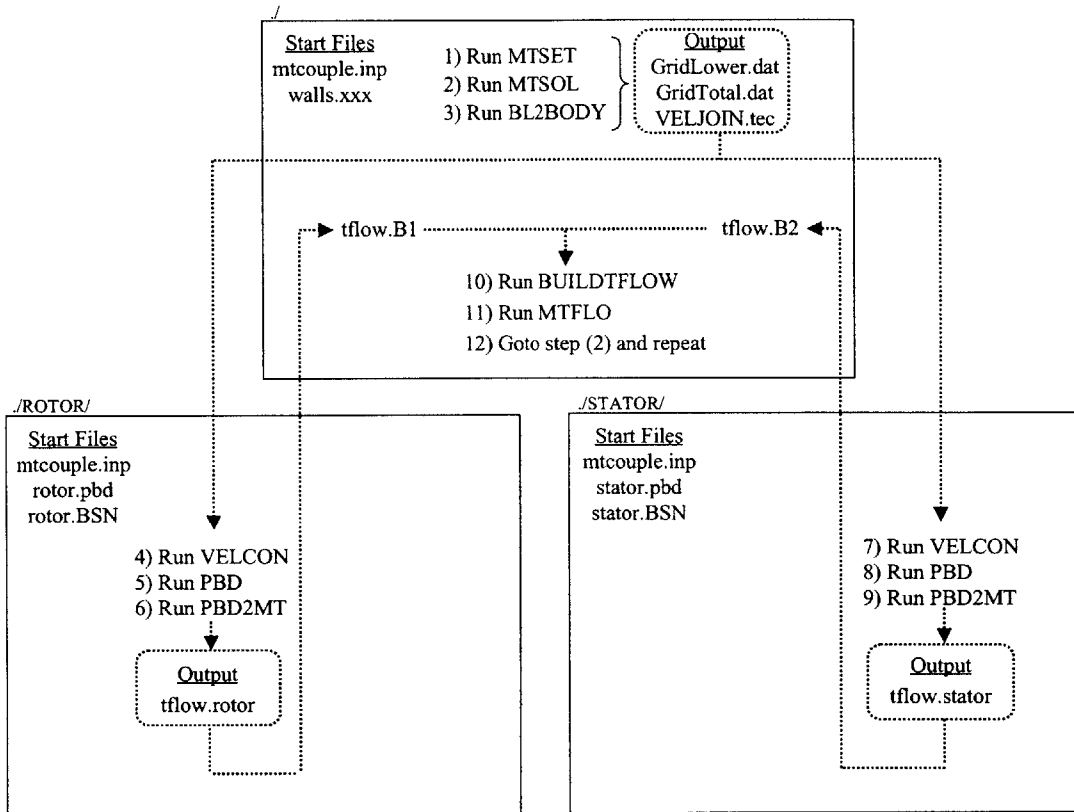


Figure 3-5: Multiple blade row coupling directory structure and program flow chart. The process is best controlled by a batch script file.

contained in Appendix A.

The final `tflow.xxx` file for a waterjet is shown in Figure 3-6. Due to the point density on the blades, the multiple points appear almost solid. Moving left to right through the flow field, the inlet *s*-line is shown first, followed by the closely spaced rotor *s*-lines containing the rotor generated  $rV_\theta$ . The mid-stage *s*-lines represent the wake from the rotor. The second set of closely spaced *s*-lines represent the stator, with their associated  $rV_\theta$  being the superposition of the rotor wake and the negative swirl induced by the stator. The outlet section is the combined rotor/stator wake, and as the stator is designed to remove the induced swirl of the rotor, this final wake exhibits only a small amount of swirl.

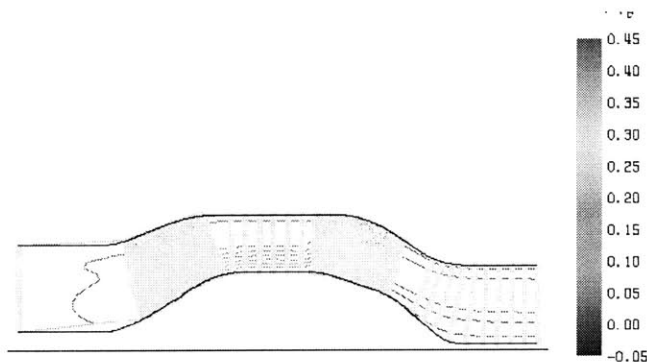


Figure 3-6: Screen capture of MTFLO displaying the `tflow.xxx` file information for a rotor/stator waterjet.

### 3.4 Upstream Boundary Layer

An additional feature of the coupled PBD/MTFLOW method, is the ability to model only the stern portion of the body of interest. This has several advantages, some of which are helpful for rapid design trade-off studies, and some of which are required to successfully model vehicles with a significant portion of the propeller within a boundary layer. The idea is to only grid, and spend computational effort, on the stern of the vehicle. The MTFLOW domain inlet is located forward of the propeller by at least two propeller diameters. Experimental data indicates that the presence of the propeller does not affect the flowfield forward of this point. Thus this size flow domain is the minimum required to adequately capture the effective wake[5]. Once the appropriate region is gridded by MTSET, the presence of a boundary layer at the inlet to the domain is modeled by adding an entropy loss in each streamtube. MTFLOW is then run in the inviscid mode, but with the boundary layer captured as an entropy loss. While the boundary layer is assumed to convect and evolve appropriately as the shape of the body changes, the additional viscous drag effects (which would normally thicken the boundary layer) occurring between the inlet plane and the propeller plane are not included in the inviscid mode. However, this effect is considered minimal in comparison to the overall accuracy and speed of this coupled method, especially given the fact that the action of the rotating blade rows will tend to accelerate the fluid and cancel much of the additional boundary layer thickness due to

friction.

Once the nominal flow is calculated, the propulsor induced swirl may be added, and the total flow field/propeller problem solved iteratively. The speed of this “stern only” method permits a rapid analysis of multiple propulsor configurations for design space exploration. The other significant advantage of this feature, is that MTFLOW can now model the contribution to the flow field by the portion of the propeller within the boundary layer displacement thickness. If run as designed, a significant portion of the propulsor on a submerged body would be within the displacement thickness, which, by definition is outside the MTFLOW domain. The desired nominal profile may be provided by other flow solvers, such as RANS, experimental data, if available, or MTFLOW itself may be used to model the full body and run in the viscous mode.

### 3.4.1 Velocity to Entropy Conversion

To convert a velocity profile into an entropy distribution, we start with the entropy equation:

$$S = \ln \left[ \frac{h_o^{\left(\frac{\gamma}{\gamma-1}\right)}}{p_o} \right] \quad (3.5)$$

For small changes (low Mach limit),

$$\Delta S = \frac{-\Delta p_o}{p_o} = -\frac{1}{2} \rho \frac{(U_o^2 - u^2)}{p_o} \quad (3.6)$$

Using the relation,

$$\rho U^2 = \gamma p M^2 \quad (3.7)$$

and, for the case of low Mach numbers (*i.e.* water) assume that the pressure is approximately equal to the absolute total pressure

$$p \approx p_o \quad (3.8)$$

so that



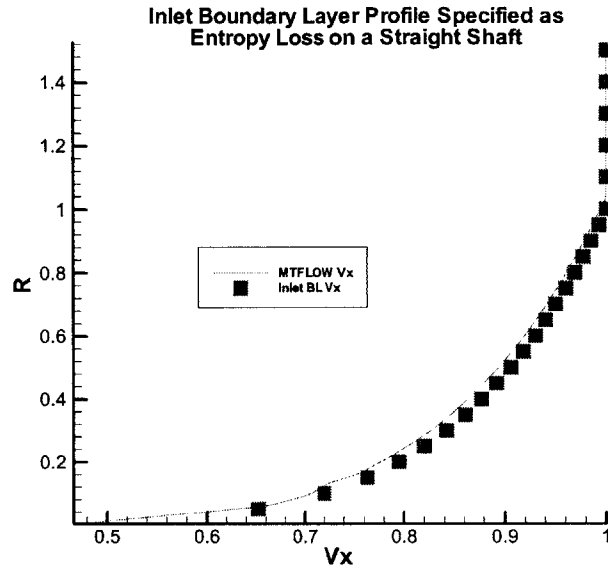


Figure 3-7: Straight shaft with  $\frac{1}{7}^{th}$  power law boundary layer specified by an entropy loss.

$$\Delta S = -\frac{1}{2}\gamma M^2 \frac{(U_o^2 - u^2)}{U_o^2} \quad (3.9)$$

While the use of the specific heat ratio,  $\gamma$ , and Mach number,  $M$ , with water flow are admittedly foreign, their use is important to correctly couple with MTFLOW. A specific heat ratio corresponding to that of air,  $\gamma = 1.4$ , is required to ensure consistency with the built in MTFLOW methodology. The Mach number is as specified in the coupling administration file, `mtcouple.inp`.

To validate the use of entropy as a boundary layer modeling tool, a straight shaft test case was conducted with a  $\frac{1}{7}^{th}$  power law boundary layer present. The results are demonstrated in Figure 3-7. The agreement between the desired boundary layer, and that convected through MTFLOW, displays the effectiveness of simulating a boundary layer as an entropy loss.

### 3.4.2 Boundary Layer Entropy Modeling on Submerged Body

When the same procedure is conducted on a body of revolution, the boundary layer profile at the domain inlet matches the specified profile, but the boundary layer downstream develops differently than the experimentally measured profile. This is presumably a result of the increasing invalidity of the pressure assumption of Equation 3.8 as the curvature of the body increases. However, to ensure that only velocity data is required for the case setup, it is not desirable to introduce a pressure correction. To overcome this deficiency, a procedure is available to tune the specified inlet velocity profile, and the associated added entropy loss, to result in the correct nominal flow field in the propeller plane. Thus, while the resultant inlet flow domain may differ from the measured profile there, as the flow develops the correct nominal profile is present in the region of the propeller. Once the necessary inlet profile is determined, it remains constant for use with the propeller present.

The procedure and program used to scale the inlet boundary layer to achieve the desired nominal profile at the propeller is displayed in Figure 3-8. Haung Body 1 (DTMB Model 5225-1) was used to validate this approach [8]. The file format of the boundary layer profiles, `BLin.txt` at the domain inlet and `Exp977nom.dat` at the propeller plane, are shown in Table 3.3. `MTFLOW` will correctly determine the radial velocity component based on the body shape, so only the axial velocity component must be specified in the boundary layer profile files. The boundary layer  $\Delta S$  loss, is added in the same manner as the blade induced  $rV_\theta$  and appears as an `MTFLO` input variable `DS` as shown in Table 3.2. The `BLINPUT TOGGLE` in the coupling administration file `mtcouple.inp` must be set to 1 to include the  $\Delta S$  loss. During the setting of the inlet profile to match the desired nominal profile at the propeller plane, a `PBDOUT.CMV` file is required to specify the blade location; however, no  $rV_\theta$  is desired. This too is controlled by the `mtcouple.inp` file by setting the `NOMINAL VELOCITY TOGGLE` to 1 during this scaling. To prevent overshooting the desired profile, a damping coefficient of 0.25 is included in each scaling step. The scaling is accomplished for each streamline as follows:

$$V_{BLin}(\psi)_{new} = V_{BLin}(\psi)_{old} \times \left[ 1 - \frac{1}{4} \left( \frac{V_{MTFLOW}(\psi) - V_{Desired}(\psi)}{V_{MTFLOW}(\psi)} \right) \right] \quad (3.10)$$

where

NumPts	
R(1)	V(1)
R(2)	V(2)
R(3)	V(3)
. . . . .	. . . . .
R(NumPts)	V(NumPts)

Table 3.3: Required format of boundary layer file. The number of points in the boundary layer are listed in the first line, followed by each R, V point, where V is the axial velocity component.

- $V_{BLin}(\psi)_{new}$   $\equiv$  updated streamline axial velocity in boundary layer input file `BLin.txt`
- $V_{BLin}(\psi)_{old}$   $\equiv$  previous streamline axial velocity in boundary layer input file `BLin.txt`
- $V_{MTFLOW}(\psi)$   $\equiv$  streamline axial velocity at propeller plane in `MTFLOW`
- $V_{Desired}(\psi)$   $\equiv$  streamline desired axial velocity at propeller plane in file `Exp977.nom`

Validation of this method was conducted with Huang Body 1 (DTMB Model 5225-1). Figure 3-10 shows the required inlet profile which results in the current boundary layer in the propeller plane shown in Figure 3-9. The complete stern section of the body and boundary layer growth is shown in Figure 3-11. Of note, a far field setting of a constant pressure jet boundary in `MTSOL` was required for stable convergence. This is imposed by setting the far field type to “3” in the solution parameter settings.

### 3.4.3 Gridding Requirements for Stern Section Modeling

The automatic gridding procedure contained in `MTSET` was designed for wings, ducts, or internal flow. Consequently, when directly applied to the stern section of a submerged body, the grid smoothing routines may have difficulty in the inlet region adjacent to the body. The bottom left corner may drift above the next streamline as shown in the top of Figure 3-12. By introducing a spline break as a doubly specified body point as demonstrated in Reference [1], and artificially lowering the inlet body point slightly, correct gridding is accomplished. This ensures the bottom streamtube has positive area, and thus an initial positive velocity. The initial grid is viewed in the `TECPLOT` formatted file `ORGGRID.tec`. The existence of a negative

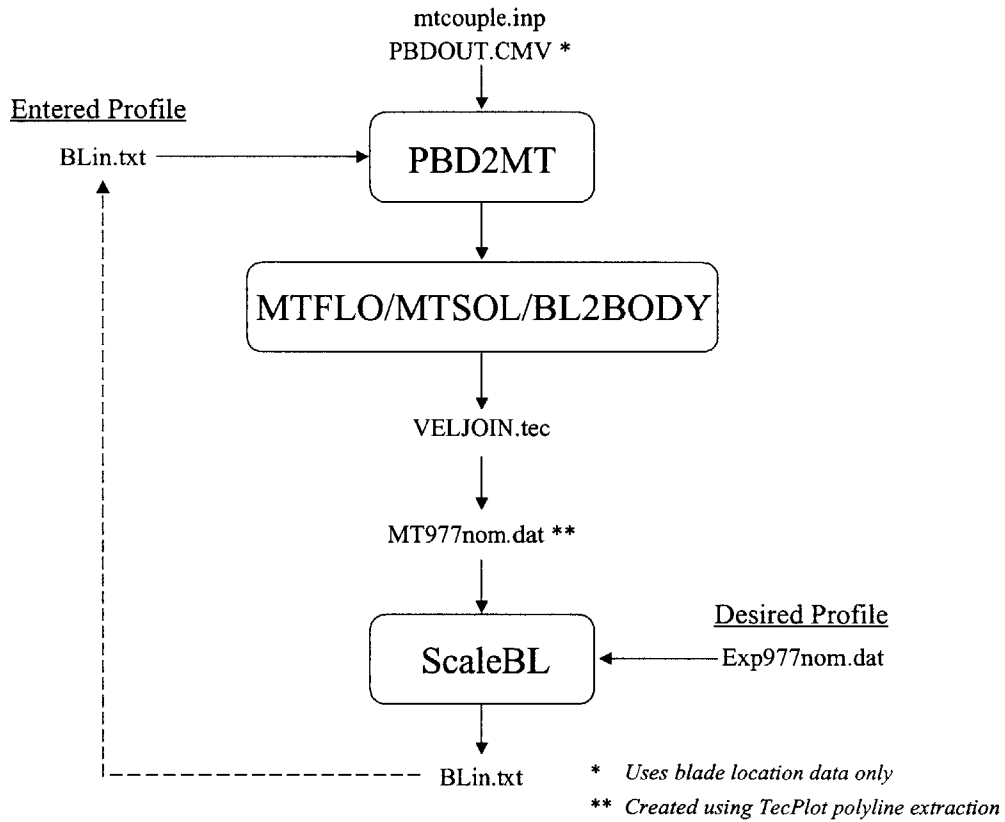


Figure 3-8: Program operation and file passing to scale the specified entropy loss to match the desired nominal profile at the propeller inlet plane.

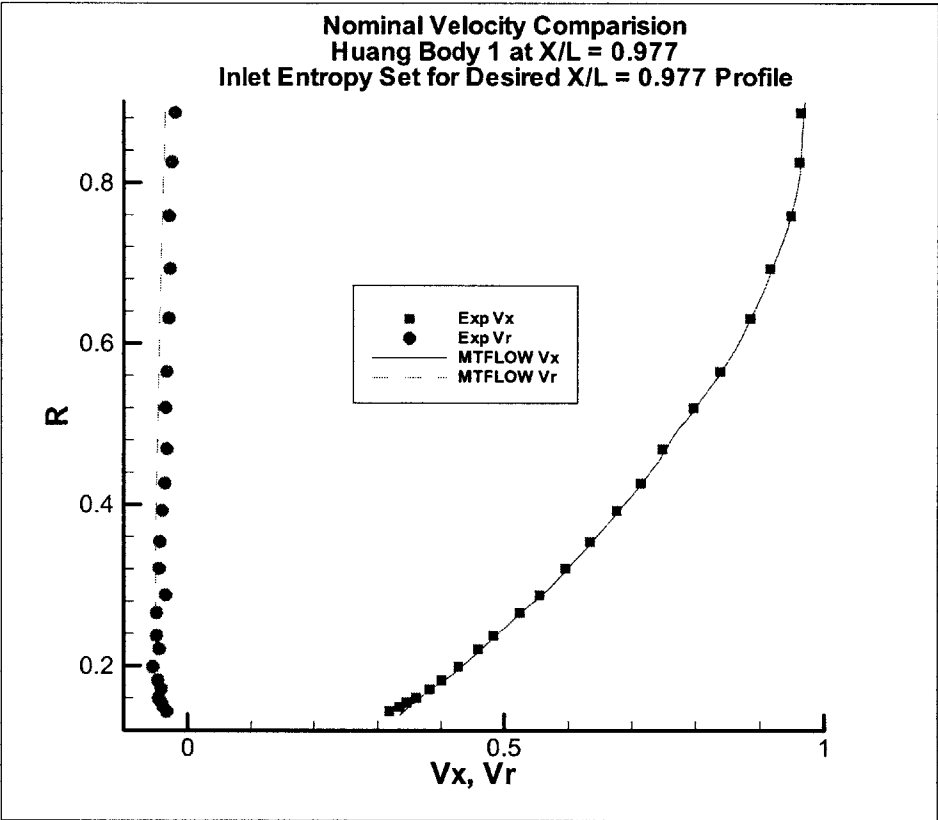


Figure 3-9: MTFLOW and experimental nominal velocity comparison of Huang Body 1 at X/L = 0.977 with inlet entropy loss specified at X/L = 0.914.

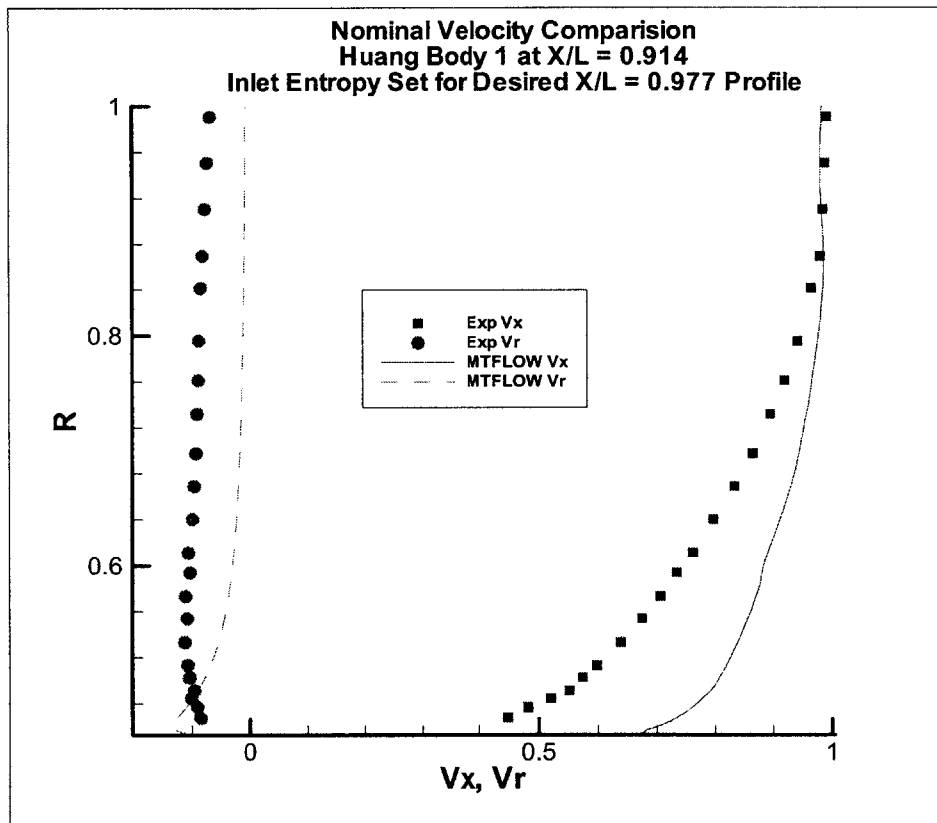


Figure 3-10: Resulting nominal velocity profile at  $X/L = 0.914$  in MTFLOW with the required entropy loss to correctly match the nominal profile at the propeller location of  $X/L = 0.977$  compared to experimental profile at  $X/L = 0.914$ .

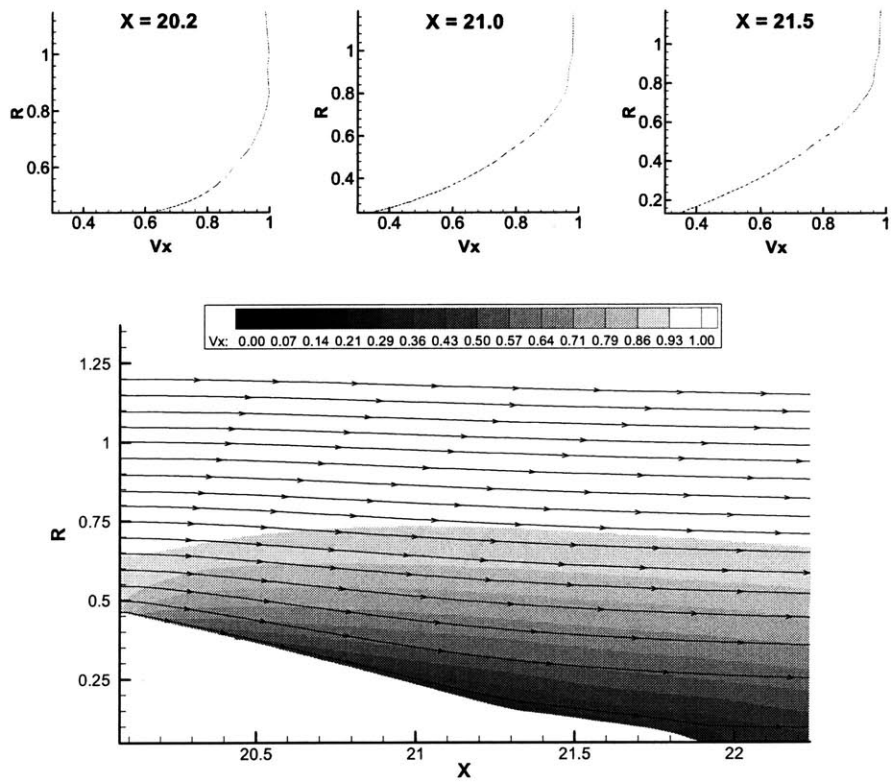


Figure 3-11: Nominal flow over stern section of Huang Body 1 with inlet boundary layer modeled as an entropy loss.

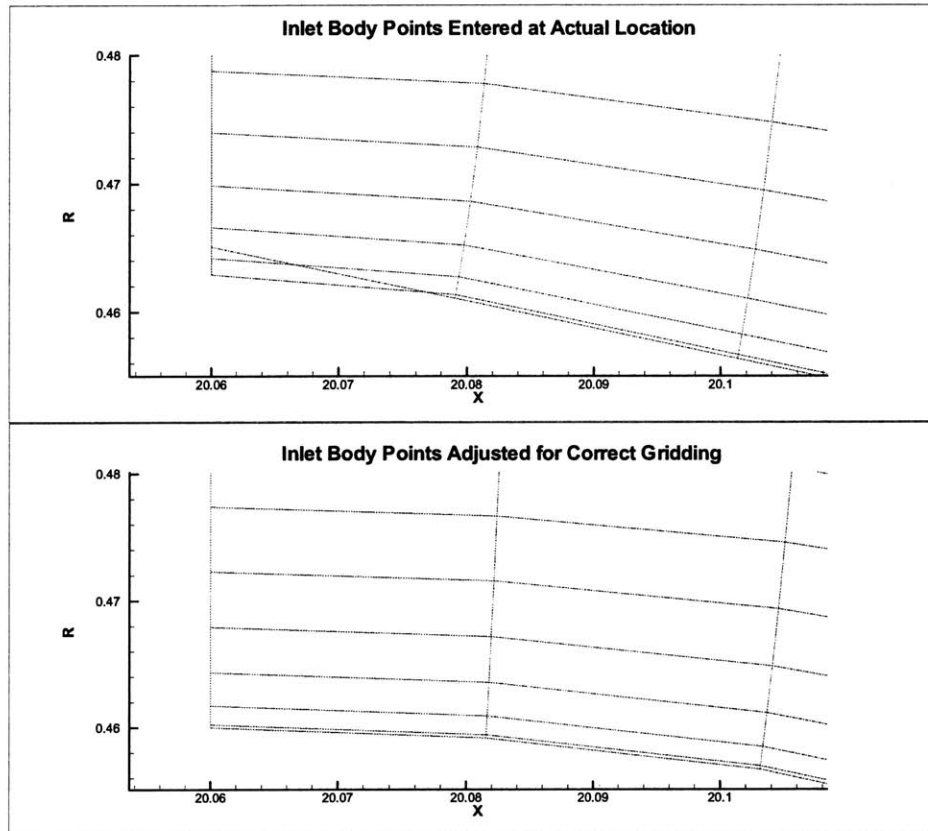


Figure 3-12: Grid comparison showing drift of bottom left corner (top) when inlet body points entered at actual location versus adjusted body points (bottom).

area can at a minimum result in localized flow difficulty, and in the extreme, can lead to a negative temperature and the subsequent crashing of the program MTSOL. Fortunately, once a successful grid is created, it is sufficient for all subsequent coupled runs. A corrected grid is shown in the bottom half of Figure 3-12. The localized point adjustment has no impact to the overall flow downstream in the propeller region.



## Chapter 4

# MTFLOW to PBD Conversions

### 4.1 Program Overview

The link from MTFLOW to PBD is accomplished by the program BL2BODY. The output from BL2BODY is the Tecplot<sup>®</sup> formatted flow field velocity file, `VELJOIN.tec`, which is read by VELCON [4], the traditional velocity conversion program used to create the updated flow field for use by PBD. For an inviscid case, BL2BODY simply converts the MTFLOW output to the correct format required by VELCON. In a viscid case, the MTFLOW output only contains inviscid velocities for a body offset by the displacement thickness, and thus the flowfield must be expanded to the body boundary, and an appropriate boundary layer velocity profile reconstructed.

### 4.2 Program Operation

The overall program execution order is displayed in Figure 4-1. The coupling administration file, `mtcouple.inp`, is read to determine whether a viscid or inviscid case exists. If the specified Reynolds number is less than ten, an inviscid case is assumed. For the inviscid case, the `VELJOIN.tec` file is written with the velocities referenced to free stream velocity, based on the velocity and Mach number as referenced in the coupling administration file. For a viscid case, a boundary layer reconstruction occurs. The beginning and ending points of the bodies, and the number of total bodies in the flow field, are determined from the `walls.xxx` file. The body

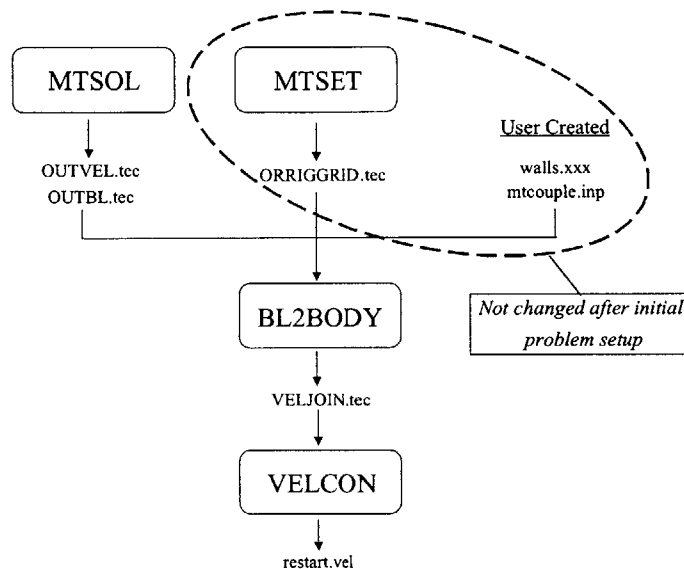


Figure 4-1: Program order and file passing when running MTFLOW to PBD. The end product is the TECPLOT format file `restart.vel` (or other name as specified during `VELCON` execution), which is the required input for PBD.

geometry is read from the `ORRIGGRID.tec` file. As this file is created by `MTSET`, before a flow solution is created, this grid conforms to the actual body location. The original work by Renick [14] utilized a Swafford boundary layer profile, however, the present coupling reverted to a pure  $\frac{1}{7}^{th}$  power law reconstruction. While this is less accurate in high pressure gradient regions, it is more robust, and was thus more consistent with the goal of a rapid, stable, automatic coupling method. Certainly, the addition of a more advanced, yet robust boundary layer reconstruction technique would improve the coupling accuracy. Of note, the recommended, and often necessary method of characterizing a boundary layer due to the presence of a significant displacement thickness in the propeller region for a viscous case, is the entropy loss method described in Section 3.4.2. When a boundary layer is created using an entropy loss, `MTFLOW` is run in the inviscid mode, and the drawbacks of the  $\frac{1}{7}^{th}$  power law are irrelevant.

The velocity output from `MTSOL` is written in the file `OUTVEL.tec`, and for a viscous case, the boundary layer information is written in the file `OUTBL.tec`. A sample `OUTVEL.tec` velocity

field is shown in Figure 4-2. The maximum displacement thickness,  $max \delta^*$ , is determined from the `OUTBL.tec` file, and following the derivation in Section 1.3.2, the maximum boundary layer thickness,  $max \delta_{99}$ , is calculated by Equation 1.18. The streamline immediately outside the  $max \delta_{99}$  is considered the lowest fully inviscid streamline. The MTFLOW grid is cut at this location, and boundary layer reconstruction is conducted between the body and the lowest fully inviscid streamline. First, new high density grid lines are faired in between the lowest fully inviscid streamline and the body. Then, velocities are assigned to the new grid nodes. If an individual node is above the local  $\delta_{99}$ , then the `OUTVEL.tec` grid is interrogated to determine the local velocities. If an individual node is between the body and the local  $\delta_{99}$  then the local axial and radial velocity components are calculated in accordance with the  $\frac{1}{7}^{th}$  power law of Equation 1.17. Between the local  $\delta^*$  and local  $\delta_{99}$  the tangential velocity is assigned the value in the MTFLOW domain as contained in `OUTVEL.tec`. Between the body and the local  $\delta^*$  no tangential velocity data exists within MTFLOW. To reasonably approximate the tangential velocity in this region, the tangential velocity is linearly interpolated between the actual value at the edge of the MTFLOW domain,  $\delta^*$ , and an assumed value at the wall of 50 % of that at the edge. Figure 4-3 shows an example `VELJOIN.tec` file written by `BL2BODY` with the new viscous, dense grid joined to the `MTSOL` calculated fully inviscid grid region.

To compare the boundary layer reconstruction with the experimental data, velocity profiles were extracted from the converged viscous Huang Body 1 nominal profile case. Figure 4-4 shows the results at four  $X/L$  locations. As expected, the  $\frac{1}{7}^{th}$  power law fails to accurately represent the experimental profile in the tapered stern section. However, it still serves as a useful tool in the absence of more detailed information, and for use along straight shafts, ducts, and internal flow cases.

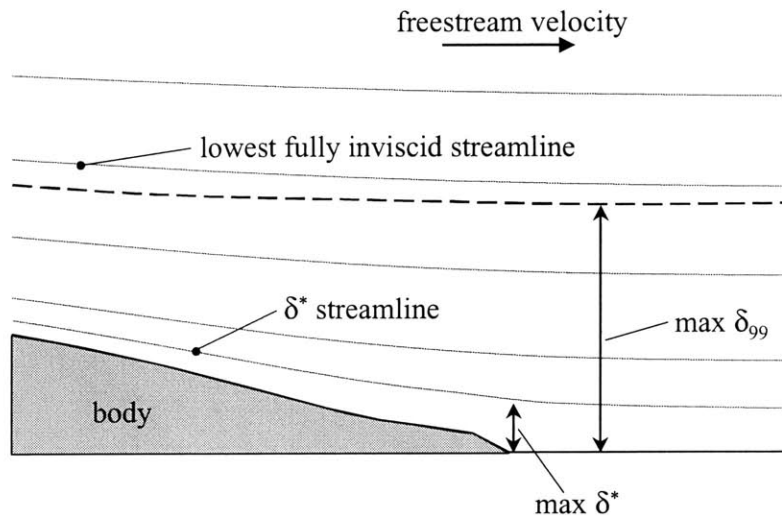


Figure 4-2: Sample viscous flowfield output from MTFLOW.

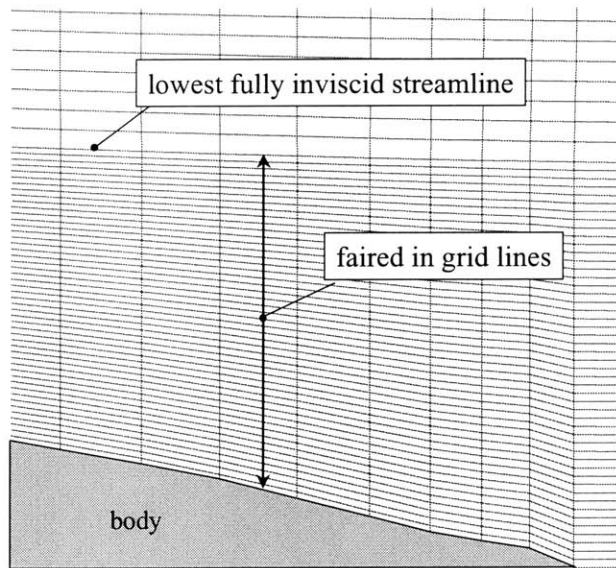


Figure 4-3: Sample BL2BODY grid with boundary layer reconstruction grid added to the inviscid MTFLOW grid.

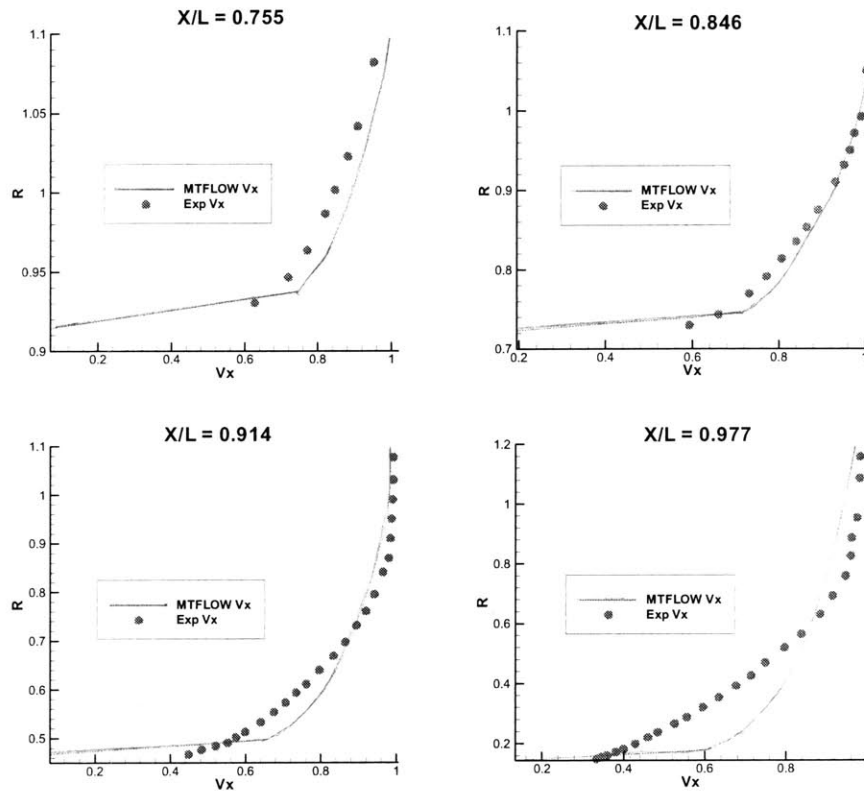


Figure 4-4: Comparison of reconstructed boundary layer profile and experimental measurements for Huang Body 1. As expected, the accuracy of the  $\frac{1}{7}^{th}$  power law diminishes in the highly tapered stern region.

# Chapter 5

## Validation

Code validation was conducted on the following cases:

1. Open Propeller
2. Ducted Propeller
3. Waterjet
4. Submerged Body

The open water comparison used propeller 4119 in comparison with the 1998 International Towing Tank Committee (ITTC) tests[13]. The ducted propeller KA-455 from the Netherland Ship Model Basin (NSMB), Kaplan series ducted propulsor [16], was utilized for the ducted case. Internal flow was validated by the WaterJet-21, as tested in the Marine Hydrodynamics Laboratory (MHL) at the Massachusetts Institute of Technology (MIT)[10]. Huang Body 1 (DTMB Model 5225-1) with propeller 4577 [5] was used for the submerged axisymmetric body comparison.

### 5.1 Open Propeller

Propeller 4119 on a straight shaft was used as the initial validation of the coupling method. Additionally, the final results were compared with the experimental results from the 1998 ITTC tests as the open propeller test case [13]. The inviscid axial effective velocity was calculated

and is show in Figure 5-1. Given a nominal axial inflow of 1.0, the axial effective inflow velocity should be equal to 1.0 on the entire blade. The near unity results demonstrate the effectiveness of the coupling method. An additional useful coupling check is to compare the tangential trailing edge velocities between PBD and MTFLOW. This is synonymous with comparing the circulation distributions. Thus, the trailing edge circumferential mean induced tangential velocities output from PBD are compared to the tangential velocity at the same spacial location in the MTFLOW calculated flow domain. This is shown in Figure 5-2. The exact agreement between both domains is an important verification that the coupling is being carried out correctly. Propeller 4119 results are compared with the 1998 ITTC experiment results in Figure 5-3. MTFLOW was run in the viscous mode, allowing boundary layer growth on the shaft. PBD was run with both the sectional drag coefficients and thickness effects included. A relatively dense lifting-surface grid of 35 x 35 vortices was required for grid convergence<sup>1</sup>. As expected, the accuracy of the solution diverges at off design  $J$  values due to the inability of the lifting surface method to adequately handle extreme blade angles-of-attack.

## 5.2 Ducted Propeller

A ducted propulsor validation was conducted using the Kaplan KA-455 with nozzle 20 as tested in the Netherlands Ship Model Basin[16]. For comparative purposes, the thrust value contains only the rotor generated thrust, and does not contain the nozzle effect. Figure 5-4 is the KA-455 as modeled in the lifting surface tool. MTFLOW was run for both an inviscid and viscid case. Once again, the PBD analysis included both the sectional drag coefficients and thickness effects. The results are shown in Table 5.1. The results demonstrate the accuracy of the method and the minimal effect that the viscous boundary layer on the shaft and duct have on the overall solution.

---

<sup>1</sup>Grid convergence means that a further increase in the grid density does not affect the results.

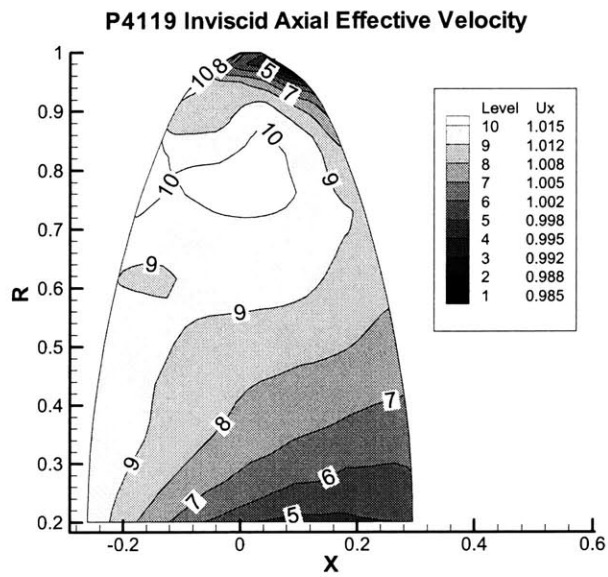


Figure 5-1: Contour plot of the effective axial velocity in the presence of a uniform nominal inflow velocity of 1.0 for P4119 on an inviscid straight shaft.

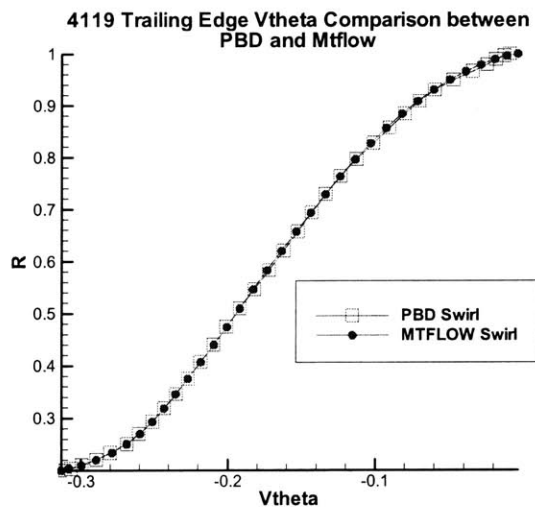


Figure 5-2: Comparison of the circumferential mean tangential velocity at the blade trailing edge of P4119 from MTFLOW and PBD.



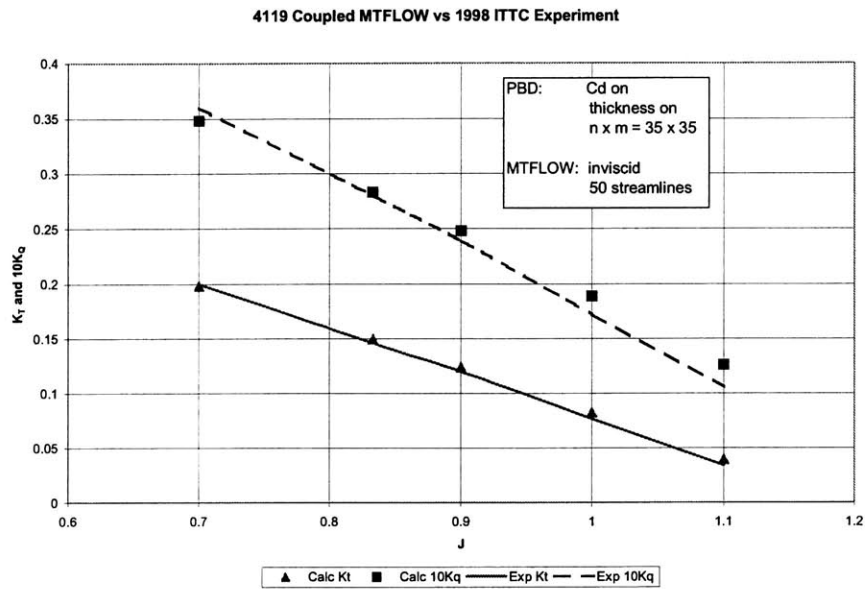


Figure 5-3: Comparison of P4119 MTFLOW/PBD results with 1998 ITTC Experiment. PBD was run with both sectional drag coefficients and thickness effects included and with a vorticity grid lattice of 35 x 35.

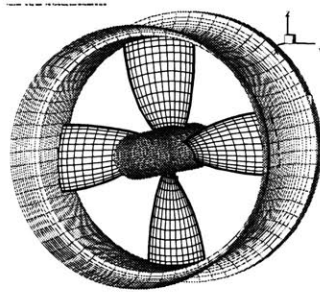


Figure 5-4: Kaplan KA-455 ducted propulsor as modeled in PBD.

	MTFLOW/PBD	MTFLOW/PBD	Experimental
<b>Re</b>	inviscid	500,000	
<b><math>K_T</math></b>	0.248	0.244	0.245
<b><math>10K_Q</math></b>	0.397	0.392	0.400

Table 5.1: Comparison of KA-455 inviscid and viscid MTFLOW/PBD rotor results with experimental data at design  $J=0.36$ .

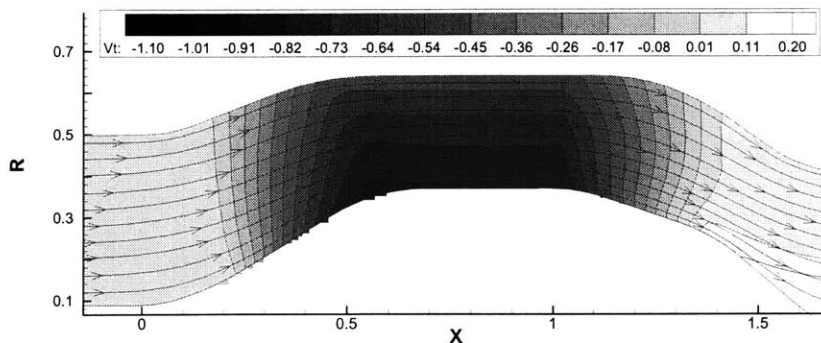


Figure 5-5: Contour plot of circumferential mean tangential velocity of WaterJet WJ21 with streamlines superimposed. Flow is from left to right. The rotor leading edge is located at approximately  $X = 0.2$  and the stator leading edge is located at approximately  $X = 1.0$ .

### 5.3 WaterJet

Internal flow verification utilized the Waterjet WJ21 tested in the Marine Hydrodynamics Laboratory at the Massachusetts Institute of Technology[10]. The torque and thrust of the rotor were compared to an equivalent RANS calculation and with the experimentally measured torque. As with the ducted case, the thrust of the rotor does not correspond to the net thrust produced by the propulsion system, but does serve as a useful quantitative comparison. A plot of the circumferential mean tangential velocities with streamlines superimposed is displayed in Figure 5-5. The results, including a computational time comparison, are shown in Table 5.2. This particular case demonstrates the relative usefulness of the MTFLOW/PBD method. The results are quite close, in spite of the fact that this is a particularly complex flow case. The reduction in computing time from 12 hours to 30 minutes is very substantial. As the flow in the test section of the waterjet is dominated by potential flow, this case was run in the inviscid mode. For design applications, the boundary layer growth of the upstream flowpath would be perfectly suited to be modeled via an entropy loss. This would permit the blade design to be conducted within the actual flow field expected, while not requiring the complete gridding of the piping system as is currently required by RANS methods.

	MTFLOW/PBD	RANS/PBD	Experimental
$K_T$	1.92	1.87	
$K_Q$	0.409	0.396	0.424
Time	30 min	12 hours	

Table 5.2: Comparison of waterjet WJ21 MTFLOW/PBD and RANS/PBD results with experimental data.

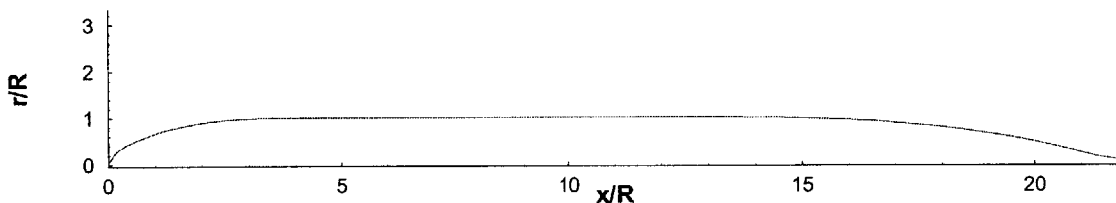


Figure 5-6: Representation of Huang Body 1 (DTMB Model 5225-1).

## 5.4 Submerged Body

This test case is one of a series of axisymmetric bodies tested by the David Taylor Model Basin by Huang et al [7], [8], [6], [5]. The same forebody (DTMB Model 5225) was used for all experiments while a series of afterbodies with an increasing degree of taper. These bodies have been used extensively for validating solutions to the effective wake problem using analytic and numerical methods. The afterbody considered here, Afterbody 1, is a non-separating stern with a low tailcone angle. A profile view of the experimental body (DTMB Model 5225-1) is shown in Figure 5-6. It was tested in the presence of an open rotor in wind tunnel and towing tank facilities. An existing seven-bladed propeller (P4577), with a diameter of 54.5 % of the hull diameter is mounted at  $x/L = 0.983$ . As the actual body boundary layer displacement thickness includes a significant portion of the propeller, the entropy loss method of Section 3.4.2 is used in this application.

To correctly set the nominal profile, experimental boundary layer profiles were selected at two locations. The first, located at  $X/L = 0.914$ , served as the initial inlet plane profile, and the second, located at the propeller inlet of  $X/L = 0.977$ , served as the goal nominal profile. The inlet plane profile was then adjusted in accordance with the procedure of Section 3.4.2 until the MTFLOW nominal propeller plane inlet profile matched the experimental profile. Once set,

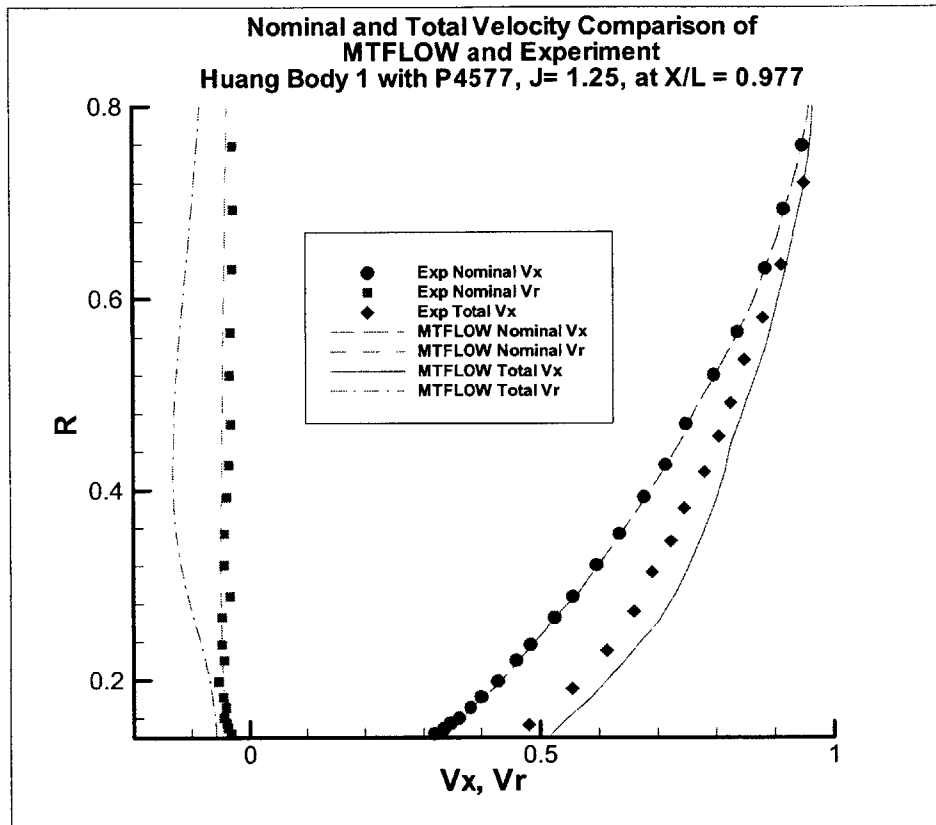


Figure 5-7: Huang Body 1 nominal and effective velocity comparison of MTFLOW and experiment at  $X/L = 0.977$  with inlet entropy loss specified at  $X/L = 0.914$ . The propeller leading edge tip is located at  $R = 0.545$ .

the inlet profile remained fixed during the propeller analysis. The nominal and total propeller plane profiles are shown in Figure 5-7. The calculated and experimental thrust and torque coefficients are contained in Table 5.3. Of note, the listed experimental torque coefficient is not purely a measured value. The propulsor used in the self-propulsion experiment was a stock propulsor and was not operated at its design angle of attack. The experimental  $K_Q$  was calculated by a propulsor performance prediction computer program based on hydrodynamic pitch angles  $\tan \beta_i$  which were iteratively scaled based on the ratio of measured to predicted  $K_T$ [5].

<sup>2</sup>A propulsor performance prediction computer program was used to compute the values of non-dimensional

	$K_T$	$K_Q$	% Error $K_T$	% Error $K_Q$
<b>Experimental<sup>2</sup></b>	0.2276	0.0453		
<b>MTFLOW/PBD-14.3</b>	0.2392	0.0436	5.1%	-3.7%

Table 5.3: Comparison of propeller 4577 performance on Huang Body 1 with  $J = 1.25$ .

The level of accuracy for Huang Body 1 is consistent with the use of PBD/MTFLOW as a rapid, early-stage, design space exploration tool. Capturing the effective wake problem in this manner allows the rapid analysis or design of multiple propellers in minutes versus hours, as is expected with RANS methods.

---

circulation  $G$  and hydrodynamic pitch angle  $\tan \beta_i$  for the estimated values of  $u_e$ . The final values of  $\tan \beta_i$  were scaled up or down by the ratio of the measured value of  $K_T$  to the computed value of  $K_T$ . The values of  $G$  and modified  $\tan \beta_i$  were then used to compute the propulsor-induced velocities by a field-point velocity computer program with a lifting-surface option. The new values of  $u_a$  were then used to compute a second estimate of the effective velocity  $u_e$ . Three iterations were sufficient for convergence[4].

# Chapter 6

## Conclusions

### 6.1 Summary of Results

The coupled PBD/MTFLOW propeller blade design and analysis method is a viable alternative to axisymmetric RANS codes for solving circumferential mean throughflow problems at a significantly reduced computational, as well as user-preparation, time. The limited number of required starting files and the automatic gridding routine of MTSET permits rapid problem set-up. The coupling works for open, ducted, and internal flow cases; for both single and multiblade rows.

### 6.2 Recommendations for Future Work

1. Addition of blade blockage effects in MTFLOW. A feature of the tflow.xxx file allows blade thickness to be passed into MTFLOW to model blockage, and thus this is an ideal feature to add to the PBD2MT program. The blockage effect becomes important for internal multi-blade propulsors.
2. Addition of viscous blade drag in MTFLOW. In the current coupling method, the viscous blade effects are accounted for by PBD in the torque and thrust calculations, however the effect of this loss on the fluid velocity is not passed back into MTFLOW. The effect of the loss is small on single-blade row open propellers, but becomes significant for multi-blade row internal flow propulsors. Accounting for this loss would improve the accuracy

of the solution in general, and would permit a realistic design capability for downstream blade rows in particular.

3. Fully automated inlet boundary layer profile modeling. The current inlet boundary layer profile method requires some user iteration to establish the entropy loss necessary to achieve the desired nominal profile. Altering the current scaling technique to a fully automatic version, transparent to the user, would further reduce the required user set-up time and level of difficulty. This is particularly beneficial in that the modeling of the stern section of a vehicle is presumably one of the most useful aspects of this coupling method, and is thus a feature which will presumably be frequently utilized.
4. Improved gridding for stand alone stern section. The gridding routine requires some manual iteration as discussed in Section 3.4.3. Eliminating this necessity would reduce the required set up time for stern section modeling.
5. Coupled Propeller Lifting Line (PLL)/MTFLOW. Coupling PLL and MTFLOW would result in a powerful design tool. The optimum circulation distribution could be designed by PLL in the effective wake as calculated by MTFLOW. Then, the blade shape design could be accomplished with PBD/MTFLOW.

# Appendix A

## Multi-Blade Row Script File

### Examples

This appendix contains example script files for a multi-blade row case. A script file for a single blade row application is a simplified version of the BatchFile below and is thus not included here.

#### A.1 BatchFile

```
TESTDIR=$HOME/RUNS/WJ
ROTOR=$TESTDIR/ROTOR
STATOR=$TESTDIR/STATOR
bl2body=$HOME/CODES/MTCouple/bl2body
velcon9=$HOME/CODES/VELCON/VELCON9/velcon9
pbd143=/nfs/propnut/CODES/CODES/PBD14/PBD14.3/SRC/pbd14
pbd2mt=$HOME/CODES/MTCouple/pbd2mt
mtflo=$HOME/CODES/Mtflow/bin/mtflo
mtsol=$HOME/CODES/Mtflow/bin/mtsol
buildtflow=$HOME/CODES/MTCouple/buildtflow
cd $TESTDIR
rm Batch.log
```



```

date > $TESTDIR/Batch.log
pwd >> $TESTDIR/Batch.log
MAX=10
COUNT=1
echo 'TITLE = ''WJ21 PBD/MTFLOW STATOR COUPLING'' >> $TESTDIR/CTQOUT.TOT
echo 'VARIABLES = ''N'', ''Ct'', ''10Cq'' >> $TESTDIR/CTQOUT.TOT
echo 'ZONE T=''Ct / 10Cq'', I= '$MAX >> $TESTDIR/CTQOUT.TOT
echo 'TITLE = ''WJ21 PBD/MTFLOW ROTOR COUPLING'' >> $TESTDIR/KTQOUT.TOT
echo 'VARIABLES = ''N'', ''Kt'', ''10Kq'' >> $TESTDIR/KTQOUT.TOT
echo 'ZONE T=''Kt / 10Kq'', I= '$MAX >> $TESTDIR/KTQOUT.TOT
cd $TESTDIR
#####
while test $COUNT -le $MAX
do
echo ' ## PBD - MTFLOW ITERATION ' $COUNT >> Batch.log
echo ' ##### PBD - MTFLOW ITERATION ' $COUNT ' #####'
#####
# MTFLOW TO PBD #
#####
# Create VELJOIN.tec from Mtf flow results
$bl2body >> Batch.log
echo ' ## Done with bl2body ##'
# Run velcon and pass req'd files to ROTOR and STATOR directories
$velcon9 < velcon.rot >> Batch.log
mv rotor.vel $ROTOR/.
cp GridLower.dat $ROTOR/.
cp GridUpper.dat $ROTOR/.
cp GridTotal.dat $ROTOR/.
cp VELJOIN.tec $ROTOR/.
$velcon9 < velcon.stat >> Batch.log

```

```

mv stator.vel $STATOR/.
cp GridLower.dat $STATOR/.
cp GridUpper.dat $STATOR/.
cp GridTotal.dat $STATOR/.
cp VELJOIN.tec $STATOR/.
#####
# PBD / PBD to MTFLOW #
#####
# Run PBD14.3 on Rotor and create tflow.rotor
cd $ROTOR
$pbid143 < pbd.in >> ../Batch.log
echo ' ## PBD complete on rotor ##'
$pbid2mt >> ../Batch.log
cp tflow.rotor $TESTDIR/tflow.B1
#cat PBDOUT.CMV >> PBDTOT.CMV
#cat PBDOUT.CMF >> PBDTOT.CMF
#cat PBDOUT.SGR >> PBDTOT.SGR
cat PBDOUT.KTQ >> ktrot.tot
tail -1 PBDOUT.KTQ > $TESTDIR/ktq.in
read word1 word2 word3 word4 < $TESTDIR/ktq.in
echo $COUNT $word3 $word4 >> $TESTDIR/KTQOUT.TOT
# Run PBD14.3 on Stator and create tflow.stator
cd $TESTDIR/STATOR
$pbid143 < pbd.in >> ../Batch.log
echo ' ## PBD complete on stator ##'
$pbid2mt >> ../Batch.log
cp tflow.stator $TESTDIR/tflow.B2
#cat PBDOUT.CMV >> PBDTOT.CMV
#cat PBDOUT.CMF >> PBDTOT.CMF
#cat PBDOUT.SGR >> PBDTOT.SGR

```

```

cat PBDOUT.KTQ >> ctstat.tot
tail -1 PBDOUT.KTQ > $TESTDIR/ktq.in
read word1 word2 word3 word4 < $TESTDIR/ktq.in
echo $COUNT $word3 $word4 >> $TESTDIR/CTQOUT.TOT
#####
# MTFLOW #
#####
# Combine tflow files and run Mtflow
cd $TESTDIR
$buildtflow >> Batch.log
echo ' ## wrote tflow.wj21 ##'
$mtflo wj21exps < runMTFLO >> Batch.log
$mtsol wj21exps < runMTSOL >> Batch.log
#####
COUNT='expr $COUNT + 1'
# End of while loop
done

```

## A.2 RunMTFLO

```
p  
r  
[return]  
[return]  
w  
q  
[return]
```

## A.3 RunMTSOL

```
x  
1  
1  
1  
1  
1  
1  
0  
w  
q  
[return]
```

## A.4 velcon.rot

```
VELJOIN.tec  
rotor.vel  
0.12396 0.52176  
1  
10  
46
```

38

0

# Bibliography

- [1] M. Drela, *A User's Guide to MTFLOW 1.2*. MIT Fluid Dynamics research Laboratory, November 1997.
- [2] M. Drela and M. Giles. Conservative Streamtube Solution of Steady-State Euler Equations. Technical Report CFDL-TR-83-6, Department of Aeronautics and Astronautics, Massachusetts Institute of Technology, November 1983.
- [3] David S. Greely and Justin E. Kerwin. Numerical Methods for Propeller Design and Analysis in Steady Flow. *SNAME Transactions*, 90:415-453, 1982.
- [4] N.J. Hahn, A.M. Polsenberg, D.H. Renick, T.E. Taylor, and J.E. Kerwin. PBD-14.3: A Coupled Lifting-Surface Design/Analysis Program for Marine Propulsors. Technical Report, Department of Ocean Engineering, Massachusetts of Technology, April 2000.
- [5] T.T. Huang and N.C. Groves. Effective Wake: Theory and Experiment. Presented at the 13th Symposium on Naval Hydrodynamics, Tokyo, Japan, October 1980.
- [6] T.T. Huang and B.D. Cox. Interaction of Afterbody Boundary Layer and Propeller. Symposium on Hydrodynamics of Ship and Offshore Propulsion Systems, Hovik Norway, March 1977.
- [7] T.T. Huang, H.T. Wang, N. Santelli, and N.C. Groves. Propeller/Stern/Boundary-Layer Interaction on Axisymmetric Bodies: Theory and Experiment. Technical Report DTNSRDC 76-0113, David W. Taylor Naval Ship Research and Development Center, December 1976.

- [8] T.T. Huang, N. Santelli, and G. Belt. Stern Boundary-Layer Flow on Axisymmetric Bodies. Presented at the 12th Symposium on Naval Hydrodynamics, Washington, DC, 1979.
- [9] J.E. Kerwin, D.P. Keenan, S.D. Black, and J.G. Diggs. A Coupled Viscous/Potential Flow Design Method for Wake-Adapted, Multi-Stage, Ducted Propulsors Using Generalized Geometry. *SNAME Transactions*, 102:23-56, 1994.
- [10] R. Kimball. In progress PhD thesis experimental results, Massachusetts Institute of Technology, Department of Ocean Engineering, 2000.
- [11] Gerard P. McHugh. Advances in Ducted propulsor Analysis Using Vortex-Lattice Lifting-Surface Techniques. Naval Engineer Thesis, Massachusetts Institute of Technology, Department of ocean Engineering, 1997.
- [12] G.P. McHugh, T.E. Taylor, W.M. Milewski, and J.E. Kerwin. PBD-14.4: A Coupled Lifting-Surface Design/Analysis Code for Marine Propulsors. Technical Report, Department of Ocean Engineering, Massachusetts of Technology, August 1998.
- [13] ITTC. 22nd ITTC Propulsion committee Propeller RANS/Panel Method Workshop. International Towing Tank Committee, 1998.
- [14] D.H. Renick. An Analysis Procedure for Advanced Propulsor Design. Naval Engineer Thesis, Massachusetts Institute of Technology, Department of Ocean Engineering, 1999.
- [15] T.W. Swafford. Analytical Approximation of Two-Dimensional Separated Turbulent Boundary-Layer Velocity Profile. *AIAA Journal*, 21:93-925, June 1983.
- [16] J.D. Van Manen. Effect of Radial Load Distribution on the Performance of Shrouded Propellers. Read at the Spring Meeting of The Royal Institution of Naval Architects, London, 1962.
- [17] F.M. White. *Viscous Fluid Flow*. McGraw-Hill, 2nd edition, 1991.